applicability of protein therapy from the middle ear space, new technology is required to overcome the difficulty of delivering large molecules to the inner ear. The Tat protein of HIV-1 is a protein of 101 residues. The Tat protein has the characteristic that it can cross the plasma membrane of neighboring cells.[31] TAT comprises the short stretches of the Tat protein domain that are primarily responsible for their translocation ability, also referred to as protein transduction domains.[32] Although the exact mechanism has not been elucidated, two models have been proposed: energy-dependent macropinocytosis, and direct uptake by electrostatic interactions and hydrogen bonding.[33] By fusing FNK to the TAT domain, FNK was effectively absorbed into the outer epithelium cells and then secreted to the inner ear space, although further studies are needed to confirm this. When fused with TAT, various proteins were reported to be transported across cell membranes.[7,8] Even β-galactosidase, whose molecular weight is 120 kDa, has been reported to enter cells.[33] Moreover, oligonucleotide, nucleic acids and liposome can also be conjugated with TAT to improve its penetration.[34] Thus, protein transduction technology allows the use of macromolecules for therapeutic application in a variety of inner ear disorders.

In our previous study, we successfully delivered TAT-FNK protein to the inner ear by intraperitoneal injection.[13] However, systemic administration may not be suitable for treatment of inner ear disorders because only relatively small amounts of drug can enter the inner ear, which therefore requires the application of high doses of drug to maintain a therapeutic concentration in the inner ear at an optimal time. Moreover, a single administration has a short half-life, as shown in our previous study,[13] and thus repeated administration is required. High doses of drug may easily induce systemic toxicities and acute allergic side effects. In particular, high doses of this antiapoptotic protein may promote tumor, although this has not been reported. Therefore, injection of drugs topically into the middle ear space may be more appropriate to better control local drug delivery. Injection of drugs into the middle ear space, however, may result in a large portion of the drug being absorbed by the middle ear mucosa or drained into the epipharynx by the Eustachian tube.[35]

To deliver a drug more effectively into the inner ear, using an absorbable material as a drug carrier may be promising. These materials could secure the stability of drugs on the RWM, and thereby lengthen the contact time with the RWM, and reduce diffusion into the mucosa and drainage from the middle ear space.[36] In the current study, we used a gelatin sponge as a carrier of TAT-FNK, as Husmann *et al*.[37] used a gelatin sponge on the RWM to topically apply gentamicin, which then induced severe damage to the cochlea compared with a single application. Similarly, Okamoto *et al*.[38] used a gelatin sponge containing bone morphogenetic protein-2, and demonstrated that bone morphogenetic protein-2 was slowly released and induced successful regeneration of cartilage in a canine tracheomalacia model. Compared with our previous systemic study,[13] we could observe immunoreactivity of TAT-myc-FNK in the cochlea using approximately 1/600th the amount of TAT-myc-FNK. Immunoreactivity of TAT-myc-FNK could still be observed in the cochlea after 24 h, which is significantly longer than the expression periods observed in previous systemic injection studies targeting organs, including the cochlea.[11,13] Further, the amount of TAT-FNK we topically applied to protect HCs from ototoxicity was approximately 1/15th the dose we used systemically to protect from the same ototoxicity in our previous study.[13] Thus, a gelatin sponge is considered to be an effective drug carrier for inner ear disorders.

When drugs are topically applied onto the RWM, they diffuse from the basal end of the cochlea and thus initially show a concentration gradient, decreasing toward the apex. The concentration gradient in the perilymph was investigated, and the greater concentration was demonstrated at the basal turn.[39,40] However, when the patterns of distribution of the drugs applied on the RWM were investigated by immunocytochemistry, the drugs appeared to be widely and rapidly distributed into the various organs of the inner ear. Imamura and Adams[40] examined the distribution of gentamicin in the inner ear of guinea pig using a monoclonal antibody. When gentamicin was placed on the RWM, the entire cochlear cell was diffusely stained until 6 h after administration. Beginning at 6 h after application, staining was found to be localized mainly in the basal turn. Greater staining in the basal turn was also found when gentamicin was administered systemically. These results suggest that gentamicin can be diffused rapidly into the entire cochlea, and that the localization of staining in the basal turn is due to the nature of the cells in the basal turn to accumulate the drug, and not because of the predominant distribution of gentamicin at the basal turn. Zou *et al*.[42] examined the distribution of lipid nanocapsules in cochlear cells after application on the RWM by using fluorescein isothiocyanate and rhodamine-B labeling. The lipid nanocapsules were present in the SGCs, OC and SV 30 min after application. Moreover, the nanocapsules were more strongly distributed in the SV in the second turn than in the basal turn. They assumed that after penetrating the RWM, the nanocapsules are rapidly diffused through the porous modiolar wall of the scala tympani, after which they enter the SGCs, and then are widely diffused through its nerve fibers. In the present study, although there was a trend of higher intensity of immunoreactivity of TAT-myc-FNK at the basal turn, we did not observe statistically significant differences among the turns. We assume that this rapid and relatively even distribution of TAT-FNK throughout the cochlea was achieved by this radial diffusion through the modiolus, and not by longitudinal perilymph diffusion. Pathways to uptake lipid nanocapsules and TAT-mediated particles into the tissue might be similar, as their high permeability is considered to accelerate their rapid diffusion.[41,42] High immunoreactivity in the SGCs compared with those in the SV and SL at 6 h can support this argument, although the cause of the higher immunoreactivity in the OC compared with that in the SGCs needs to be clarified in future research.

It is known that high-frequency hearing loss occurs initially after AG ototoxicity. However, when the damage by AG is severe, apical cells will be affected and hearing loss expands to lower frequencies.[43] The doses of the KM and EA combination we chose were assumed to be sufficient to cause threshold shifts even at a low frequency. We observed some tendency that the OHCs in the basal parts are more susceptible to the combination of EA and KM than those the upper parts (Figures 4a and b). This finding is consistent with that in other studies.[44] When we compared the extent of missing HCs in the region corresponding to the frequency at which ABR was measured, the percentages of missing OHCs was approximately 67% in the region corresponding approximately to 4 kHz and 80% in that corresponding to 20 kHz. In untreated ears, the percentages of missing OHCs in the regions comparable to 4 and 20 kHz were 95% and 100%, respectively. The differences in the extent of OHC loss between the 4- and 20-kHz regions were small, supporting the ABR findings that there was no significant difference in the threshold shifts among the tested frequencies, although the ABR threshold shifts were slightly greater at higher frequencies than at lower frequencies.

In the current study, we showed that caspase-9 was activated by KM *in vitro*. This finding suggests that KM-induced cochlear HC death is caspase-9-dependent, which is consistent with other studies.[1,45] We demonstrated that TAT-FNK suppressed the activation of caspase-9 in this study and reduced the extent of cleaved PARP in OHCs in our previous study,[13] which suggests that TAT-FNK prevents the intrinsic apoptotic pathway, as does the parent protein Bcl-x_L. It has also been shown that TAT-FNK affects the cytosolic movement of Ca^{2+} and protects neuronal cells from glutamate excitotoxicity.[11] It has been shown *in vitro* that AG antibiotics cause an increase in intracellular calcium levels

in avian HCs[46] and in isolated OHCs of guinea pigs.[47] Therefore, inhibition of Ca^{2+} homeostasis distribution may have a crucial role in the ability of TAT-FNK to prevent apoptotic cochlear HC death. The mechanism of how TAT-FNK prevents cochlear HC death remains to be fully elucidated.

In conclusion, we demonstrated that TAT-FNK infiltrated in gelatin sponge and placed on the guinea pig RWM could successfully deliver the protein to the cochlea by penetrating through the RWM, and that a single topical administration of TAT-FNK protected the cochlea against the combination of the ototoxic drugs KM and EA *in vivo*. An *in vitro* study demonstrated that TAT-FNK suppressed the activation of caspase-9 and protected cochlear HCs from KM-induced apoptosis. These findings suggest that topical administration of an antiapoptotic protein fused with TAT and soaked with a gelatin sponge is effective at preventing the apoptosis of cochlear HCs, and that such topical treatment is superior to systemic administration in terms of organ specificity and safety. Future studies using this technology may extend the feasibility of protein therapy for treatment of inner ear disorders.

MATERIALS AND METHODS

The experimental protocol was approved by the University Committee for the Use and Care of Animals at the University of Tokyo, and it conforms to the NIH Guidelines for the Care and Use of Laboratory Animals.

Construction and preparation of TAT-FNK and TAT-myc-FNK

We constructed FNK (originally designated as Bcl-xFNK) by introducing amino-acid substitutions into Bcl-x_L using a two-step PCR mutagenesis method, as reported previously.[9] The substituted codons were as follows: Tyr-22 (TAC) with Phe (TTC), Gln-26 (CAG) with Asn (AAC) and Arg-165 (CGG) with Lys (AAG). Among the mammalian antiapoptotic factors, FNK is the only mutant with a gain-of-function phenotype because, compared with Bcl-x_L, FNK showed stronger antiapoptotic activity to protect cultured cells from death induced by various death stimuli, including oxidative stress, a calcium ionophore and withdrawal of growth factors.[9] TAT-FNK and TAT-myc-FNK were then prepared as described previously.[11] The gene constructed for FNK was fused with an oligonucleotide encoding TAT, and the resulting TAT-FNK gene encoded met-gly-TAT (consisting of 11 amino acids: YGRKKRRQRRR)-gly-FNK. An oligonucleotide encoding GEQKLISEEDLG (the myc TAG sequence is underlined) was inserted between the TAT and FNK sequences of TAT-FNK by PCR to obtain TAT-myc-FNK. To construct myc-FNK without the TAT domain, an oligonucleotide encoding met-gly-myc TAG-gly was also ligated to the FNK sequence by PCR. The TAT-FNK plasmid was introduced into *Escherichia coli* DH5a cells (Invitrogen, Life Technology, Carlsbad, CA, USA) and the TAT-FNK protein was overexpressed by treatment with 1 mM isopropyl 1-thio-β-D-galactoside for 5 h with vigorous shaking at 37 °C. Proteins were solubilized in buffer (7 M urea, 2% sodium dodecyl sulfate, 1 mM dithiothreitol, 62.5 mM Tris-HCl (pH 6.8) and 150 mM NaCl) and then subjected to sodium dodecyl sulfate-PAGE to remove contaminating proteins and endotoxins. The gel was treated with 1 M KCl and the transparent band corresponding to TAT-FNK was cut out. Proteins were electrophoretically extracted from the gel slice using extraction buffer (25 mM Tris, 0.2 M glycine and 0.1% sodium dodecyl sulfate) for *in vitro* and *in vivo* experiments. The extraction buffer was used as the vehicle. The concentration of the extracted TAT-FNK ranged from 1 to 6 mg ml^{-1}.

Immunohistochemical detection of TAT-myc-FNK in the cochlea after tympanic administration

Eighteen male albino guinea pigs (Saitama Experimental Animals Supply Co. Ltd, Saitama, Japan) weighing 250–300 *g* were used. Under anesthesia with xylazine hydrochloride (10 mg kg^{-1}; Bayer, Leverkusen, Germany) and ketamine hydrochloride (40 mg kg^{-1}; Sankyo, Tokyo, Japan), a postauricular incision was made and the bone posterior to the tympanic ring was exposed. A hole was drilled into the bulla exposing the middle ear space medial to the tympanic ring. The round window niche and the RWM were identified. The gelatin sponge (Spongel; Astellas Pharma Inc., Tokyo, Japan) was soaked in 3 μl of TAT-myc-FNK (0.5 mg ml^{-1}) and placed on the RWM of the left ear. The animals were killed at 1, 3, 6, 12, 24 and 48 h ($n = 3$ for each time point) after injection, while under deep anesthesia, using an overdose of xylazine hydrochloride (Bayer) and ketamine hydrochloride (Sankyo). Three animals that were killed 6 h after a similar tympanic administration of myc-FNK (3 μl; 0.5 mg ml^{-1}) served as controls. The cochleae from both ears were perfused with 4% paraformaldehyde in 0.1 M phosphate-buffered saline (PBS) at pH 7.4 through the oval and round windows, and immersed in the same fixative overnight at 4 °C. The specimens were decalcified in 10% EDTA acid for 14 days, dehydrated through a graded alcohol series and embedded in paraffin. The embedded tissues were cut into 5-μm-thick sections parallel to the modiolus and mounted on glass slides. The sections were deparaffinized, hydrated and rinsed with PBS. To detect TAT-myc-FNK and myc-FNK *in situ*, rabbit an anti-myc-tag polyclonal antibody was used (1:5000, 4 °C overnight; Upstate Biotechnology, Lake Placid, NY, USA) coupled with a DAKO Envision + system (Dako Japan, Kyoto, Japan). Negative controls were established by replacing the primary antibody with blocking buffer.

The LI of the anti-myc antibody in the cochlear tissues was obtained by a modified Photoshop-based image analysis. The original method was developed by Lehr *et al.*[48] In brief, an image was digitized on magnetic optical disks. Using the 'Magic Wand' tool in the 'Select' menu of Photoshop, the cursor was placed on a portion of the immunostained area. The tolerance level of the Magic Wand tool was adjusted so that the entire immunostained area was selected. Using the 'Similar' command in the 'Select' menu, all the immunostained areas were selected automatically. Subsequently, the image was transformed to an 8-bit grayscale format. An optical density plot of the selected areas was generated using the 'Histogram' tool in the 'Image' menu. The mean staining intensity and the number of pixels in the selected areas were quantified. Next, the background was selected using the 'Inverse' tool in the 'Select' menu. The mean background intensity was quantified using the 'Histogram' tool as mentioned above. The immunostaining intensity was calculated as the difference between the mean staining intensity and the mean background intensity. The immunostained ratio was calculated as the ratio of the number of pixels in all the immunostained areas to that in the entire image. LI was defined as the product of the immunostained ratio and the immunostaining intensity. The modiolar sections were obtained in every third section and five sections were randomly selected from each ear (10 sections from each animal). As a result, the LI was measured using 30 sections in each group by a technician naïve to the treatment, preparation techniques or the aims of the current study. To investigate differences among the cochlear turns, the LIs in the basal, second and third turns were also measured 1 and 6 h after application. The LIs of the SGCs, SV and SL 6 h after the application of TAT-myc-FNK onto the RWM, as well as those in the controls, were also measured. To compare the immunostaining intensity among the cells in these organs, the ratios of normalized immunoreactivity were calculated by dividing the LIs at 6 h by those of the control.

Tympanic injection of TAT-FNK *in vivo*

Eight male albino guinea pigs, weighing 250–300 g and showing ABR thresholds within normal limits based on our laboratory database, were used in this investigation. Only male animals were used because there are gender differences in the ability to detoxify reactive oxygen species and in the levels of endogenous antioxidants in the cochlea.[49,50]

Animals were anesthetized with xylazine hydrochloride (10 mg kg^{-1}) and ketamine hydrochloride (40 mg kg^{-1}). Chloramphenicol sodium succinate (30 mg kg^{-1}, intramuscular injection) was administered as a prophylactic. Under aseptic conditions, the bulla was exposed bilaterally from an occipitolateral approach and opened to allow visualization of the RWM. A gelatin sponge soaked with 3 μl of TAT-FNK (6 mg ml^{-1}) was placed on the RWM in the left ear, whereas a gelatin sponge soaked with only a vehicle was placed on the RWM in the right ear. One hour after the wound was sutured, a single dose of KM (200 mg kg^{-1}; Meiji, Tokyo, Japan)

was injected subcutaneously. Then, 2 h after the KM injection, the jugular vein was exposed under general anesthesia and EA (40 mg kg^{-1}; Sigma-Aldrich, Tokyo, Japan) was infused into the vein as described previously.[51] An additional four animals served as drug controls: a gelatin sponge soaked with 3 μl of TAT-FNK (6 mg ml^{-1}) was placed on the left RWM, but KM and EA were not administered.

ABR measurement

ABRs were recorded using waveform storing and stimulus control using MEB-5504 (NIHON KOHODEN CO., Tokyo Japan) and DPS-725 (DIA MEDICAL CO., Tokyo, Japan). Sound stimuli were produced by the PT-R7 III ribbon-type speaker (PIONEER CO., Tokyo, Japan). Recordings were performed in a closed-field TRAACOUSTICS acoustic enclosure (TRACOUSTICS INC., Austin, TX, USA) and sound level calibration was performed using a sound-level meter (NA-28 RION, Tokyo, Japan). Pure tones (4, 8 and 20 kHz) were measured 3 days after the arrival of the animals to determine the baseline thresholds, and 14 days after the ototoxic insult (for experimental animals) or TAT-FNK application (for drug control animals) to determine the threshold shifts. The frequencies (4, 8 and 20 kHz) measured in this study were frequently used for other studies using guinea pigs, including our previous study.[13,52,53] We have limited our investigation to these frequencies to evaluate hearing to minimize the stress on these animals. The method of ABR measurement has been described previously.[54] In brief, animals were anesthetized with a mixture of xylazine hydrochloride (10 mg kg^{-1}, intramuscular) and ketamine hydrochloride (40 mg kg^{-1}, intramuscular), and needle electrodes were placed subcutaneously at the vertex (active electrode), beneath the pinna of the measured ear (reference electrode) and beneath the opposite ear (ground). The stimulus duration was 15 ms, with a presentation rate of 11 s^{-1}, and the rise/fall time was 1 ms. Responses of 1024 sweeps were averaged at each intensity level (5-dB steps) to assess the threshold. The threshold was defined as the lowest intensity level at which a clear reproducible waveform was visible in the trace. When an ABR waveform could not be evoked, the threshold was assumed to be 5 dB greater than the maximum intensity produced by the system (105 dB SPL). Threshold shifts were calculated by subtracting the baseline thresholds from those observed before killing.

Assessment of extent of HC loss

After ABR measurements 14 days after ototoxic insults (experimental animals) or TAT-FNK application (drug control animals), animals were killed under deep anesthesia using xylazine hydrochloride and ketamine hydrochloride. The bilateral cochleae were perfused with 4% paraformaldehyde in 0.1 M PBS at pH 7.4 through the oval and round windows, and then immersed in the same fixative overnight at 4 °C. The cochleae were then washed with PBS, permeabilized with 0.3% Triton X-100 for 10 min and labeled with 1% rhodamine phalloidin (Molecular Probes, Eugene, OR, USA) for 30 min to stain F-actin. The tissues were processed as whole mounts using the surface preparation technique. The specimens were then mounted on glass slides using the Prolong Antifade kit (Molecular Probes) and observed. Reticules whose length (bin width) at × 40 was 0.45 mm were used to count the numbers of total and missing HCs. HCs that showed an identifiable cell body and cuticular plate were considered to be present. The presence of distinctive scar formations produced by convergence of adjacent phalangeal processes was regarded as an indicator of a missing HC. The percentage of HC loss for the IHCs and OHCs was calculated for each segment obtained from each animal. The average for each segment was then determined for each group and plotted from the apex to the base to produce an average cytocochleogram. Two animals were excluded because of tissue damage during surface preparation, leaving a total of six cochleae for the HC count study.

Assessment of the protective effects of TAT-FNK and caspase-9 detection for cultured HCs

Sprague–Dawley rats (Saitama Experimental Animals Supply Co. Ltd) were decapitated on postnatal day 5 (P5) and the cochlea was carefully dissected out. On the basis of the methods of Sobkowicz *et al.*,[55] the SV, the SL and the spiral ganglion neurons were dissected away, leaving the OC. The cochlea used for analysis was prepared by cutting 2 mm from the basal end and 3 mm from the apical end of the cochlea (approximately half of the cochlea). Explants were maintained in Dulbecco's modified Eagle's medium with 10% fetal bovine serum, 25 mM Hepes and 30 U ml^{-1} penicillin, and were cultured in an incubator at 37 °C under 5% CO_2 and 95% humidity for 24 h. Explants were exposed to medium containing 20 nM TAT-FNK, 20 nM FNK without TAT or vehicle. Two hours after exposure, the medium was changed to one containing 6 mM KM and either 20 nM FNK, 20 nM TAT-FNK or the vehicle. Typically, 10 cultures were evaluated for each experimental condition: four were cultured for 10 h for detection of caspase-9 and six were cultured for 12 h for cell counting. Additional 10 cultures were evaluated for control, of which four were cultured for 10 h and six were cultured for 12 h, with the medium containing no KM.

Caspase-9 activity was examined by using the fluorescent caspase substrate fam-LEHD-fmk (caspase-9 substrate), which was obtained from Intergen (Purchase, NY, USA) and used according to the manufacturer's protocol. After culturing, the fluorescent substrate was added directly to the culture medium (final concentration, 5 μM) for the final hour in culture. After 1 h in this substrate, the OC was washed three times for 15 min each at 37 °C in the washing buffer supplied by the manufacturer. The cultures were then fixed overnight at 4 °C in the fixative supplied by the manufacturer. After fixation, the cochleae were washed with PBS, permeabilized with 0.3% Triton X-100 for 10 min and labeled with 1% rhodamine phalloidin (Molecular Probes) for 30 min to stain F-actin. Whole mounted cochleae were viewed with a confocal laser-scanning microscope (ZEISS LSM5 PASCAL). Caspase-9-positive cells were counted over a 0.2 mm longitudinal distance from four separate regions in each culture. A mean value was determined for each culture.

For HC counting, cultures were fixed overnight at 4 °C in the fixative supplied by the manufacturer. After fixation, the cochleae were washed with PBS, permeabilized with 0.3% Triton X-100 for 10 min and labeled with 1% rhodamine phalloidin (Molecular Probes) for 30 min to stain F-actin. To quantify HC loss in the cochlea after various treatments, IHCs and OHCs were counted over a 0.2 mm longitudinal distance from four separate regions of each culture. A mean value was determined for each culture.

Statistical analysis

The SPSS software was used for statistical analysis. The time course of the LI for TAT-myc-FNK in the OC was compared between groups by one-way and then pairwise comparisons, with statistical significance adjusted for multiple comparisons (Scheffe's test). The differences in the turns of the LI for TAT-myc-FNK in the OC at 1 and 6 h were compared by two-way ANOVA (the independent variables were cochlear turns and time course). The differences in the normalized LIs between the sub-sites in the cochlea were compared by one-way ANOVA, and then pairwise comparisons were performed by using Scheffe's test. The ABR thresholds at each frequency before and 14 days after the ototoxic insults were compared by two-way ANOVA (the independent variables were TAT-FNK administration and hearing frequency). The extent of missing HCs *in vitro* was also compared by two-way ANOVA (the independent variables were TAT-FNK treatment and type of HC). Caspase-9 activities between the groups were compared by one-way ANOVA followed by Scheffe's test. The extent of missing HCs *in vitro* after exposure to KM was compared by two-way ANOVA (the independent variables were type of HC and drug administration), and if a statistically significant interaction was observed, Bonferroni test was used for simple effects analysis. A level of $P<0.05$ was accepted as statistically significant.

CONFLICT OF INTEREST

The authors declare no conflict of interest.

ACKNOWLEDGEMENTS

We thank Ms A Tsuyuzaki and Ms Y Kurasawa (Department of Otolaryngology and Head and Neck Surgery, Faculty of Medicine, University of Tokyo, Tokyo, Japan) for technical assistance. This work was supported by Grants (17659527 and 20390440)

from the Ministry of Education, Culture, Sports, Science, and Technology of Japan to TY and a Grant (15110201) from the Ministry of Health, Labor and Welfare of Japan to TY.

REFERENCES

1 Cheng AG, Cunningham LL, Rubel EW. Mechanisms of hair cell death and protection. *Curr Opin Otolaryngol Head Neck Surg* 2005; **13**: 343 - 348.
2 Rybak LP, Whitworth CA, Mukherjea D, Ramkumar V. Mechanisms of cisplatin-induced ototoxicity and prevention. *Hear Res* 2007; **226**: 157 - 167.
3 Rizzi MD, Hirose K. Aminoglycoside ototoxicity. *Curr Opin Otolaryngol Head Neck Surg* 2007; **15**: 352 - 357.
4 Staecker H, Liu W, Malgrange B, Lefebvre PP, Van De Water TR. Vector-mediated delivery of bcl-2 prevents degeneration of auditory hair cells and neurons after injury. *ORL J Otorhinolaryngol Relat Spec* 2007; **69**: 43 - 50.
5 Liu YH, Ke XM, Qin Y, Gu ZP, Xiao SF. Adeno-associated virus-mediated Bcl-xL prevents aminoglycoside-induced hearing loss in mice. *Chin Med J* 2007; **120**: 1236 - 1240.
6 Haas R, Murea S. The role of granulocyte colony-stimulating factor in mobilization and transplantation of peripheral blood progenitor and stem cells. *Cytokines Mol Ther* 1995; **1**: 249 - 270.
7 Schwarze SR, Ho A, Vocero-Akbani A, Dowdy SF. *In vivo* protein transduction: delivery of a biologically active protein into the mouse. *Science* 1999; **285**: 1569 - 1572.
8 Becker-Hapak M, McAllister SS, Dowdy SF. TAT-mediated protein transduction into mammalian cells. *Methods* 2001; **24**: 247 - 256.
9 Asoh S, Ohtsu T, Ohta S. The super antiapoptotic factor Bcl-xFNK constructed by disturbing intramolecular polar interactions in rat Bcl-xL. *J Biol Chem* 2000; **275**: 37240 - 37245.
10 Asoh S, Mori T, Nagai S, Yamagata K, Nishimaki K, Miyato Y *et al.* Zonal necrosis prevented by transduction of the artificial anti-death FNK protein. *Cell Death Differ* 2005; **12**: 384 - 394.
11 Asoh S, Ohsawa I, Mori T, Katsura K, Hiraide T, Katayama Y *et al.* Protection against ischemic brain injury by protein therapeutics. *Proc Natl Acad Sci USA* 2002; **99**: 17107 - 17112.
12 Nagai S, Asoh S, Kobayashi Y, Shidara Y, Mori T, Suzuki M *et al.* Protection of hepatic cells from apoptosis induced by ischemia/reperfusion injury by protein therapeutics. *Hepatol Res* 2007; **37**: 133 - 142.
13 Kashio A, Sakamoto T, Suzukawa K, Asoh S, Ohta S, Yamasoba T. A protein derived from the fusion of TAT peptide and FNK, a Bcl-x(L) derivative, prevents cochlear hair cell death from aminoglycoside ototoxicity *in vivo*. *J Neurosci Res* 2007; **85**: 1403 - 1412.
14 Minn AJ, Boise LH, Thompson CB. Expression of Bcl-xL and loss of p53 can cooperate to overcome a cell cycle checkpoint induced by mitotic spindle damage. *Genes Dev* 1996; **10**: 2621 - 2631.
15 Valera ET, Brassesco MS, Scrideli CA, Tone LG. Tetraploidization in Wilms tumor in an infant. *Genet Mol Res* 2010; **9**: 1577 - 1581.
16 Schuknecht HF. Ablation therapy for the relief of Meniere's disease. *Trans Am Laryngol Rhinol Otol Soc* 1956; **66**: 589 - 600.
17 Haynes DS, O'Malley M, Cohen S, Watford K, Labadie RF. Intratympanic dexamethasone for sudden sensorineural hearing loss after failure of systemic therapy. *Laryngoscope* 2007; **117**: 3 - 15.
18 Tsuji J, Liberman MC. Intracellular labeling of auditory nerve fibers in guinea pig: central and peripheral projections. *J Comp Neurol* 1997; **381**: 188 - 202.
19 Tanaka K, Motomura S. Permeability of the labyrinthine windows in guinea pigs. *Arch Otorhinolaryngol* 1981; **233**: 67 - 73.
20 Bellucci RJ, Fisher EG, Rhodin J. Ultrastructure of the round window membrane. *Laryngoscope* 1972; **82**: 1021 - 1026.
21 Carpenter AM, Muchow D, Goycoolea MV. Ultrastructural studies of the human round window membrane. *Arch Otolaryngol Head Neck Surg* 1989; **115**: 585 - 590.
22 Mirisztai E, Benedeczky I, Horváth K, Köllner P. Ultrastructural organization of the round window membrane in the infant human middle ear. *ORL J Otorhinolaryngol Relat Spec* 1983; **45**: 29 - 38.
23 Goycoolea MV, Lundman L. Round window membrane. Structure function and permeability: a review. *Microsc Res Tech* 1997; **36**: 201 - 211.
24 Lundman LA, Holmquist L, Bagger-Sjoback D. Round window membrane permeability. An *in vitro* model. *Acta Otolaryngol* 1987; **104**: 472 - 480.
25 Juhn SK, Hamaguchi Y, Goycoolea M. Review of round window membrane permeability. *Acta Otolaryngol Suppl* 1989; **457**: 43 - 48.
26 Smith BM, Myers MG. The penetration of gentamicin and neomycin into perilymph across the round window membrane. *Otolaryngol Head Neck Surg* 1979; **87**: 888 - 891.
27 Brady DR, Pearce JP, Juhn SK. Permeability of round window membrane to 22Na or RISA. *Arch Otorhinolaryngol* 1976; **214**: 183 - 184.
28 Nomura Y. Otological significance of the round window. *Adv Otorhinolaryngol* 1984; **33**: 1 - 162.
29 Morizono T, Hamaguchi Y, Juhn SK. *Permeability of human serum albumin from chinchilla middle ear to inner ear. In XXIII workshop on inner ear biology 1986*. GDR: Berlin.
30 Goycoolea MV, Paparella MM, Goldberg B, Carpenter AM. Permeability of the round window membrane in otitis media. *Arch Otolaryngol* 1980; **106**: 430 - 433.
31 Richard JP, Melikov K, Vives E, Ramos C, Verbeure B, Gait MJ *et al.* Cell-penetrating peptides. A reevaluation of the mechanism of cellular uptake. *J Biol Chem* 2003; **278**: 585 - 590.
32 Vivès E, Brodin P, Lebleu B. A truncated HIV-1 Tat protein basic domain rapidly translocates through the plasma membrane and accumulates in the cell nucleus. *J Biol Chem* 1997; **272**: 16010 - 16017.
33 Wadia JS, Dowdy SF. Protein transduction technology. *Curr Opin Biotechnol* 2002; **13**: 52 - 56.
34 Gupta B, Levchenko TS, Torchilin VP. Intracellular delivery of large molecules and small particles by cell-penetrating proteins and peptides. *Adv Drug Deliv Rev* 2005; **57**: 637 - 651.
35 Ruel-Gariepy E, Chenite A, Chaput C, Guirguis S, Leroux J. Characterization of thermosensitive chitosan gels for the sustained delivery of drugs. *Int J Pharm* 2000; **203**: 89 - 98.
36 Park AH, Jackson A, Hunter L, McGill L, Simonsen SE, Alder SC *et al.* Cross-linked hydrogels for middle ear packing. *Otol Neurotol* 2006; **27**: 1170 - 1175.
37 Husmann KR, Morgan AS, Girod DA, Durham D. Round window administration of gentamicin: a new method for the study of ototoxicity of cochlear hair cells. *Hear Res* 1998; **125**: 109 - 119.
38 Okamoto T, Yamamoto Y, Gotoh M, Huang CL, Nakamura T, Shimizu Y *et al.* Slow release of bone morphogenetic protein 2 from a gelatin sponge to promote regeneration of tracheal cartilage in a canine model. *J Thorac Cardiovasc Surg* 2004; **127**: 329 - 334.
39 Salt AN. Simulation of methods for drug delivery to the cochlear fluids. *Adv Otorhinolaryngol* 2002; **59**: 140 - 148.
40 Imamura S, Adams JC. Distribution of gentamicin in the guinea pig inner ear after local or systemic application. *J Assoc Res Otolaryngol* 2003; **4**: 176 - 195.
41 Zou J, Saulnier P, Perrier T, Zhang Y, Manninen T, Toppila E *et al.* Distribution of lipid nanocapsules in different cochlear cell populations after round window membrane permeation. *J Biomed Mater Res B Appl Biomater* 2008; **87**: 10 - 18.
42 Khalil IA, Kogure K, Akita H, Harashima H. Uptake pathways and subsequent intracellular trafficking in nonviral gene delivery. *Pharmacol Rev* 2006; **58**: 32 - 45.
43 Chen Y, Huang WG, Zha DJ, Qiu JH, Wang JL, Sha SH, Schacht J. Aspirin attenuates gentamicin ototoxicity: from the laboratory to the clinic. *Hear Res* 2007; **226**: 178 - 182.
44 Priuska EM, Schacht J. Mechanism and prevention of aminoglycoside ototoxicity: outer hair cells as targets and tools. *J Ear Nose Throat J* 1997; **76**: 164 - 166, 168, 170-1.
45 Cunningham LL, Cheng AG, Rubel EW. Caspase activation in hair cells of the mouse utricle exposed to neomycin. *J Neurosci* 2002; **22**: 8532 - 8540.
46 Hirose K, Westrum LE, Stone JS, Zirpel L, Rubel EW. Dynamic studies of ototoxicity in mature avian auditory epithelium. *Ann NY Acad Sci* 1999; **884**: 389 - 409.
47 Li Y, Huang Y, Luo S. Alternation of intracellular Ca2+ caused by streptomycin in the isolated cochlear OHC. *Zhonghua Er Bi Yan Hou Ke Za Zhi* 1995; **30**: 227 - 229.
48 Lehr HA, Mankoff DA, Corwin D, Santeusanio G, Gown AM. Application of Photoshop-based image analysis to quantification of hormone receptor expression in breast cancer. *J Histochem Cytochem* 1997; **45**: 1559 - 1565.
49 Julicher RH, Sterrenberg L, Haenen GR, Bast A, Noordhoek J. Sex differences in the cellular defence system against free radicals from oxygen or drug metabolites in rat. *Arch Toxicol* 1984; **56**: 83 - 86.
50 el Barbary A, Altschuler RA, Schacht J. Glutathione *S*-transferases in the organ of Corti of the rat: enzymatic activity, subunit composition and immunohistochemical localization. *Hear Res* 1993; **71**: 80 - 90.
51 Yamasoba T, Kondo K. Supporting cell proliferation after hair cell injury in mature guinea pig cochlea *in vivo*. *Cell Tissue Res* 2006; **325**: 23 - 31.
52 Suzuki M, Yagi M, Brown JN, Miller AL, Miller JM, Raphael Y. Effect of transgenic GDNF expression on gentamicin-induced cochlear and vestibular toxicity. *Gene Ther* 2000; **7**: 1046 - 1054.
53 Lin CD, Oshima T, Oda K, Yamauchi D, Tsai MH, Kobayashi T. Ototoxic interaction of kanamycin and 3-nitropropionic acid. *Acta Otolaryngol* 2008; **128**: 1280 - 1285.
54 Pourbakht A, Yamasoba T. Ebselen attenuates cochlear damage caused by acoustic trauma. *Hear Res* 2003; **181**: 100 - 108.
55 Sobkowicz HM, Loftus JM, Slapnick SM. Tissue culture of the organ of Corti. *Acta Otolaryngol Suppl* 1993; **502**: 3 - 36.

Biochimica et Biophysica Acta 1820 (2012) 608–614

Contents lists available at SciVerse ScienceDirect

Biochimica et Biophysica Acta

journal homepage: www.elsevier.com/locate/bbagen

Review

Molecular pathology of MELAS and L-arginine effects☆,☆☆

Yasutoshi Koga [a,*], Nataliya Povalko [a], Junko Nishioka [a], Koujyu Katayama [a], Shuichi Yatsuga [a,b], Toyojiro Matsuishi [a]

[a] Department of Pediatrics and Child Health, Kurume University Graduate School of Medicine, Kurume, Japan
[b] Research Program of Molecular Neurology, Biomedicum Helsinki, University of Helsinki, Helsinki, Finland

ARTICLE INFO

Article history:
Received 14 April 2011
Received in revised form 7 July 2011
Accepted 7 September 2011
Available online 14 September 2011

Keywords:
Mitochondrial cytopathy
Translation
RNA 19
Angiopathy
Endothelial dysfunction
L-arginine

ABSTRACT

Background: The pathogenic mechanism of stroke-like episodes seen in mitochondrial myopathy, encephalopathy, lactic acidosis, and stroke-like episodes (MELAS) has not been clarified yet. About 80% of MELAS patients have an A3243G mutation in the mitochondrial $tRNA^{Leu(UUR)}$ gene, which is the base change at position 14 in the consensus structure of $tRNA^{Leu(UUR)}$ gene.

Scope of review: This review aims to give an overview on the actual knowledge about the pathogenic mechanism of mitochondrial cytopathy at the molecular levels, the possible pathogenic mechanism of mitochondrial angiopathy to cause stroke-like episodes at the clinical and pathophysiological levels, and the proposed site of action of L-arginine therapy on MELAS.

Major conclusions: Molecular pathogenesis is mainly demonstrated using ρ^0 cybrid system. The mutation creates the protein synthesis defects caused by 1) decreased life span of steady state amount of $tRNA^{Leu(UUR)}$ molecules; 2) decreased ratio of aminoacyl-$tRNA^{Leu(UUR)}$ versus uncharged $tRNA^{Leu(UUR)}$ molecules; 3) the accumulation of aminoacylation with leucine without any misacylation; 4) accumulation of processing intermediates such as RNA 19, 5) wobble modification defects. All of these loss of function abnormalities are created by the threshold effects of cell or organ to the mitochondrial energy requirement when they establish the phenotype. Mitochondrial angiopathy demonstrated by muscle or brain pathology, as SSV (SDH strongly stained vessels), and by vascular physiology using FMD (flow mediated dilation). MELAS patients show decreased capacity of NO dependent vasodilation because of the low plasma levels of L-arginine and/or of respiratory chain dysfunction. Although the underlying mechanisms are not completely understood in stroke-like episodes in MELAS, L-arginine therapy improved endothelial dysfunction.

General significance: Though the molecular pathogenesis of an A3243G or T3271C mutation of mitochondrial $tRNA^{Leu(UUR)}$ gene has been clarified as a mitochondrial cytopathy, the underlying mechanisms of stroke-like episodes in MELAS are not completely understood. At this point, L-arginine therapy showed promise in treating of the stroke-like episodes in MELAS. This article is part of a Special Issue entitled Biochemistry of Mitochondria.

1. Introduction

Mitochondrial myopathy, encephalopathy, lactic acidosis, and stroke-like episodes (MELAS) (OMIM 540000), characterized by an early onset of stroke-like episodes, was first described by Pavlakis and colleagues in 1984 [1]. At least 39 distinct mitochondrial DNA mutations have been associated with MELAS [2], about 80% of MELAS patients have an A3243G mutation in the mitochondrial $tRNA^{Leu(UUR)}$ gene (OMIM 590050) [3–5]. Although more than 25 years have passed since MELAS was first defined clinically and pathologically, the pathogenesis of the stroke-like episodes is still uncertain. Mitochondrial angiopathy with degenerative changes in small arteries and arterioles, which has been reported in many MELAS patients [6,7], is suggested by the observation of strong succinate dehydrogenase activity in the wall of blood vessels (SSVs) [8]. In spite of the fact that many therapeutic trials have been conducted to cure mitochondrial disorders, no trial has been successful, though several clinical trials are still on-going. Based on the hypothesis that stroke-like episodes in MELAS are caused by segmental impairment of vasodilatation in intracerebral arteries, we use L-arginine in MELAS patients during the acute phase to cure the symptoms or to

☆ This article is part of a Special Issue entitled Biochemistry of Mitochondria.

☆☆ Acknowledgment statement (including conflict of interest and funding sources): All coauthors have seen the manuscript and have reported no conflicts of interest (financial or nonfinancial) and declared all other pertinent financial information. This work was supported in part by grants #13670853 (Y.K.) and #16390308 (Y.K.) from the Ministry of Culture and Education in Japan, as well as #CCT-B-1803 (Y.K.) from Evidence-based Medicine, Ministry of Health, Labor and Welfare in Japan. S.Y. is a recipient of a post-doctoral fellowship from the Academy of Finland, the Center for International Mobility in Finland.

* Corresponding author at: Department of Pediatrics and Child Health, Kurume University School of Medicine, 67 Asahi-Machi, Kurume City, Fukuoka 30-0011, Japan. Tel.: +81 942 31 7565; fax: +81 942 38 1792.
E-mail address: yasukoga@med.kurume-u.ac.jp (Y. Koga).

0304-4165/$ – see front matter © 2011 Elsevier B.V. All rights reserved.
doi:10.1016/j.bbagen.2011.09.005

decrease the frequency and/or the severity of the stroke-like episodes [9,10,11]. This review aims to give an overview on the actual knowledge about the pathogenic mechanism of mitochondrial cytopathy at the molecular levels, the possible pathogenic mechanism of mitochondrial angiopathy to cause stroke-like episodes in the clinical and pathophysiological levels, and the proposed site of action of L-arginine therapy on MELAS.

2. Molecular pathophysiology of mitochondrial cytopathy in MELAS

2.1. Characteristics of $tRNA^{Leu(UUR)}$ gene and structure stabilization of mutant

A point mutation in the structural gene for a tRNA may be expected to result in a deficiency in translation. However, inhibition of translation due to a mutated tRNA gene may occur at several levels. The base change at position 14 in the consensus structure of $tRNA^{Leu(UUR)}$ is an invariant A in bacterial and cytosolic eukaryotic tRNAs and is typically involved in the tertiary folding of classical tRNAs (Fig. 1A) [12]. Because of above reason, the A3243G mutation is primarily thought to disrupt the tertiary interaction between the highly conserved np A14 (>90% for adenine) and U8, a binding that stabilizes the L-shaped tertiary fold [13,14], which results in partially folded tRNA transcripts into the L-shaped structure with an acceptor branch but with a floppy anticodon branch [15]. The mutant tRNA is able to adapt to the synthetase, but results in incorrect tRNA processing and enzyme maturation and accordingly defects in a variety of biochemical pathways. The mutation may directly affect the mitochondrial tRNA function in translation, such as structure stabilization, methylation, amino-acylation, and codon recognition, or alternatively, may affect recognition of the tRNA by an enzyme not directly involved in translation, such as the enzymes which process the large polycistronic transcripts of the mtDNA.

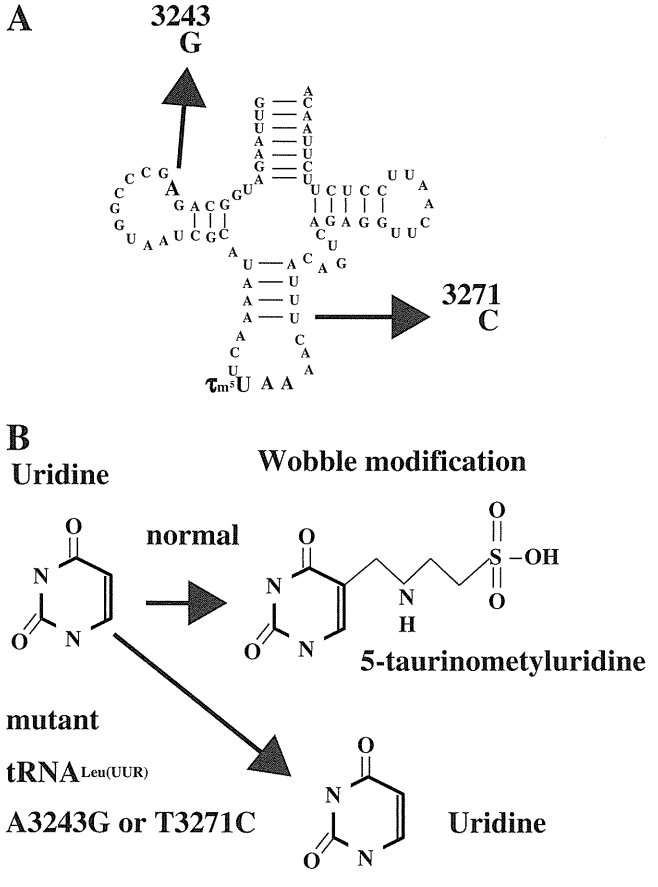

Fig. 1. $tRNA^{Leu(UUR)}$ structure and wobble modification. $tRNA^{Leu(UUR)}$ structure. An A to G change at position 14 in the consensus structure of $tRNA^{Leu(UUR)}$, which is thought to disrupt the tertiary folding of classical tRNAs [12], results in partially folded tRNA transcripts into the L-shaped structure with an acceptor branch but with a floppy anticodon branch [14,15]. B. Wobble modification The wild-type $tRNA^{Leu(UUR)}$ contains an unknown modified uridine at the wobble position and that this modification occurs at the uracil base [35], however its modification is absent in the $tRNA^{Leu(UUR)}$ with a mutation at either np A3243G or T3271C. The wobble modified uridine in the wild-type $tRNA^{Leu(UUR)}$ is 5-taurinomethyluridine (sm5U). The U on the bold indicates the unmodified uridine present in the mutant tRNAs.

2.2. ρ^0 cybrid system in MELAS

King et al. developed the technologies whereby the mitochondria from cells derived from patients are transferred to a cell line lacking mtDNA (so called ρ^0 cybrid system), which allowed to conduct the study of the genotype-phenotype relationships in mitochondrial function [16,17]. In this manner, it is possible to create trans-mitochondrial cell lines containing different proportions of mutated mtDNA from 0% to 100%, and to study the effects of a given mutant load on the activity of respiratory chain complexes, mitochondrial respiration and cell growth, as well as mitochondrial tRNA stability, methylation, aminoacylation, codon recognition and threshold effects. First application of this technique to an A3243G mutation related to molecular basis of MELAS, has been reported by Chomyn et al. [18], and King et al. [19] independently. Mutant transformants showed protein synthesis defects clearly, and demonstrated that there was the direct evidence between single nucleotide change at 14th position of an A to G transition in the mitochondrial $tRNA^{Leu(UUR)}$ gene and mitochondrial dysfunction. However, the reduction in labeling of the various mitochondrial translation products in mutant was not correlated with their UUR-encoded leucine content. King also reported the similar effects in transformants having a T3271C mutation [19]. This ρ^0 cybrid system becomes the orthodox and powerful tool when one evaluates the pathogenicity of any nucleotide changes in the mitochondrial DNA.

2.3. Transcription termination of mitochondrial RNAs in MELAS

The mammalian mitochondrial tRNAs are transcribed as part of larger polycistronic RNAs, in which the tRNA sequences are contiguous or nearly contiguous to the rRNA sequences and the protein-coding sequences (Fig. 2). The ribosomal gene region appears to be transcribed 50–100 times more frequently than the other H-strand genes [20]. In these polycistronic molecules, the tRNA structures are believed to act as recognition signals for the processing enzymes which make precise endonucleolytic cleavages at the 5' and 3' ends of the tRNA sequences in the primary transcripts, yielding the mature rRNAs, mRNAs, and tRNAs [21]. The ribosomal DNA transcription unit, one of three polycistronic transcription units of human mtDNA, terminates at the 3'-end of the 16S rRNA gene just before the $tRNA^{Leu(UUR)}$ gene. This transcript, corresponding to the ribosomal genes, is processed to yield the mature rRNAs and, due to its very high rate of synthesis, is responsible for the bulk of the rRNA formation [22]. Transcription termination is mediated by a protein factor (mTERF: mitochondrial termination factor) which specifically binds within the $tRNA^{Leu(UUR)}$ gene, and which promotes termination of transcription (Fig. 3A) [22,23]. Since this mutation is located exactly in the middle of termination protein binding domain, the A3243G mutation in the $tRNA^{Leu(UUR)}$ gene has been shown in vitro to impair the binding of this protein factor and to affect the efficiency of transcription termination at the end of the 16S rRNA gene [23]. However, in vivo analysis using ρ^0 cybrid system provided no evidence to support above data. There were no alterations of size of the $tRNA^{Leu(UUR)}$ or of the immediately downstream-encoded ND1 mRNA or of the 16S rRNA, as detectable by changes in their electrophoretic mobility [18]. The steady-state amounts of mitochondrial rRNAs, mRNAs, and $tRNA^{Leu(UUR)}$ are not significantly affected by the MELAS mutation in ρ^0 cybrid system. The discrepancy of the data described above may be explained by the possibility that the

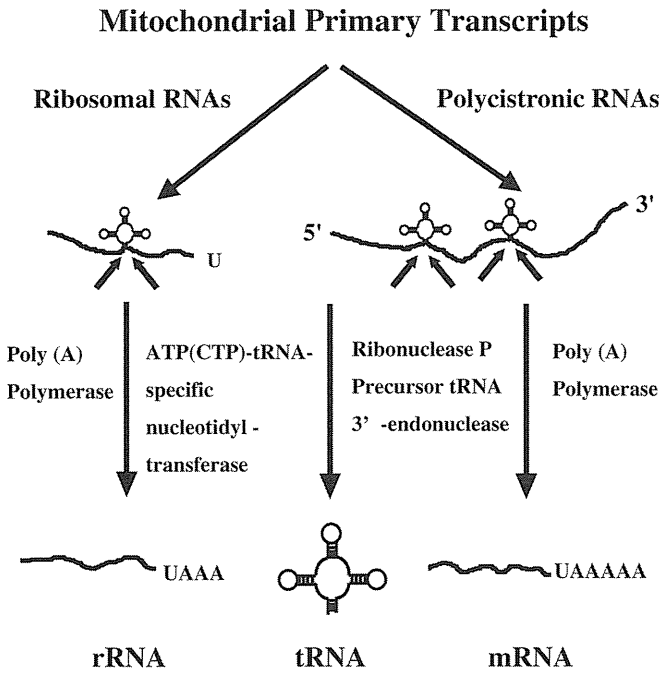

Fig. 2. Mammalian mitochondrial transcription system. The human mitochondrial RNAs are transcribed as a larger polycistronic RNAs, in which the tRNA sequences are contiguous or nearly contiguous to the rRNA sequences and the protein-coding sequences.

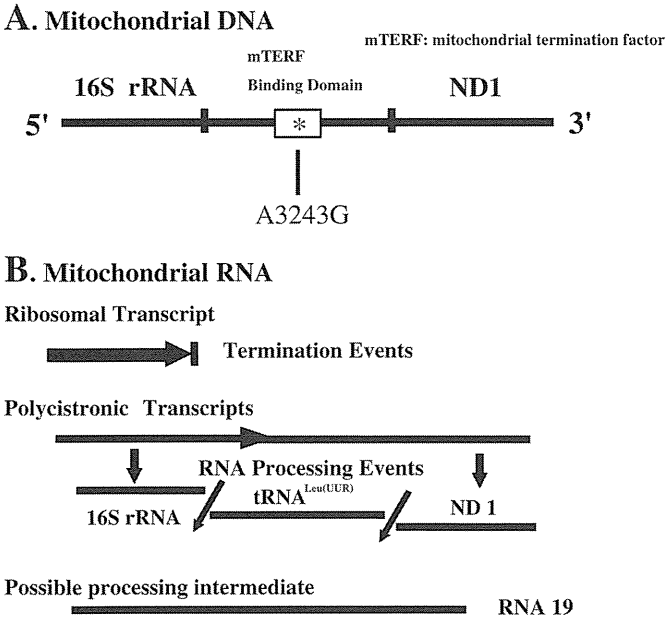

Fig. 3. Post-transcriptional modification. A. Transcription termination. The ribosomal gene region appears to be transcribed 50–100 times more frequently than the other H-strand genes [20]. Transcription termination is mediated by a protein factor (mTERF: mitochondrial termination factor) which specifically binds within the $tRNA^{Leu(UUR)}$ gene, and which promotes termination of ribosomal transcription. B. Post-transcriptional modification and RNA 19 The increase of RNA 19, corresponding to the 16S rRNA + $tRNA^{Leu(UUR)}$ + ND 1 genes, found in mutant $tRNA^{Leu(UUR)}$ cybrids clearly demonstrate that RNA processing is not occurring in mutant cybrids as efficiently as in wild-type cybrids [19]. RNA 19 is also accumulated in muscle specimens from 8 MELAS patients [26]. The proportion of mutated RNA in RNA 19 fraction is always higher than those in the percentage of mutation in mitochondrial DNA, suggesting that the A3243G mutation exhibited dominant negative effects on the mitochondrial RNA processing events, resulting in the accumulation of RNA 19 transcripts in these patients [28–30].

reduction in affinity of mTERF for the mutated target sequence is compensated by hyper-expression of the protein. Anyway, using genetic, biochemical, and morphological techniques, it was found that the mutant, but not wild-type cybrids, displayed quantitative deficiencies in cell growth, protein synthesis, and respiratory chain activity [19].

2.4. Processing of polycistronic transcripts in MELAS

It was found that there was an accumulation of a previously unidentified RNA transcript in mutant cybrids (A3243G or T3271C), designated as RNA 19, corresponds to the 16S rRNA + $tRNA^{Leu(UUR)}$ + ND1 genes, which are contiguous in the mtDNA (Fig. 3B) [19]. The ratios of mtDNA-encoded rRNAs to mRNAs were not found to be altered in these in vitro experiments. In order to analyze whether the MELAS mutation is associated with errors in transcription termination and processing of the polycistronic transcripts in the region of the mutation, it was performed fine mapping of the mature transcripts derived from the 16S rRNA, $tRNA^{Leu(UUR)}$, and ND 1 genes in both wild-type and mutant cybrids. It was also analyzed the steady-state levels of $tRNA^{Leu(UUR)}$ by high-resolution RNA transfer hybridizations. It was found that mutation has no effect in vivo on the accuracy of transcription termination at the end of the ribosomal RNA genes, on the precise endonucleolytic cleavage of the polycistronic RNA at $tRNA^{Leu(UUR)}$, or on the post transcriptional addition of -CCA at the 3′ end of $tRNA^{Leu(UUR)}$ [24]. On the other hand, the experiments using plasmids carrying $tRNA^{Leu(UUR)}$ inserts (wild type, as well as A3243G) which designated to evaluate the endonucleolytic 3′-end processing and CCA addition at the tRNA 3′ terminus, showed that A3243G mutation reduced 2.2 fold of the efficiency of 3′-end cleavage, and almost has no abnormal effects on CCA addition [25].

2.5. Accumulation of RNA 19 in MELAS cybrids and organs from patients

The increased amounts of the transcript corresponding to the 16S rRNA + $tRNA^{Leu(UUR)}$ + ND 1 genes, designated as RNA 19, found in mutant $tRNA^{Leu(UUR)}$ cybrids clearly demonstrate that RNA processing is not occurring in mutant cybrids (A3243G or T3271C) as efficiently as in wild-type cybrids [19]. It was demonstrated that RNA 19 is accumulated in muscle specimens from 8 MELAS patients who have a heterogeneous percentage of mutation (58% to 99%) in the A3243G of $tRNA^{Leu(UUR)}$ gene [26]. An increase in the levels of RNA 19 was observed in nearly all tissues examined from these patients, which do not provide evidence for tissue-specific differences in mitochondrial RNA processing. The elevation of steady-state levels of RNA 19 have also reported in skeletal muscle and fibroblasts of a patient with mitochondrial myopathy and a complex I deficiency who harbored an A to G transition in $tRNA^{Leu(UUR)}$ gene at position 3302 [27]. Thus, altered RNA processing may be associated with other point mutations in $tRNA^{Leu(UUR)}$ gene associated with MELAS. It also analyzed a mutated proportion of RNA 19 in an RNA fraction obtained from sampled skeletal muscles from 6 unrelated patients with MELAS. The proportion of mutated RNA in RNA 19 fraction exceeded 95% in all patients, although the percentage of mutation in mitochondrial DNA ranged from 54 to 92, suggesting that the A3243G mutation exhibited dominant negative effects on the mitochondrial RNA processing events, resulting in the accumulation of RNA 19 transcripts in these patients [28–30]. The protein synthesis defect has been proposed to be due to stalling of translation by pseudoribosomes that have incorporated RNA 19, an incompletely processed transcript reported to accumulate in A3243G, T3271C and A3302G mutant cells, in place of 16 S rRNA, or possibly to defective posttranscriptional modification of the $tRNA^{Leu(UUR)}$ (Fig. 4) [31]. Though the reason why RNA 19 was elevated in patients who have the point mutation of $tRNA^{Leu(UUR)}$ gene is unknown, we believe that elevated levels of RNA 19 may play an important role in the pathogenesis of this disorder.

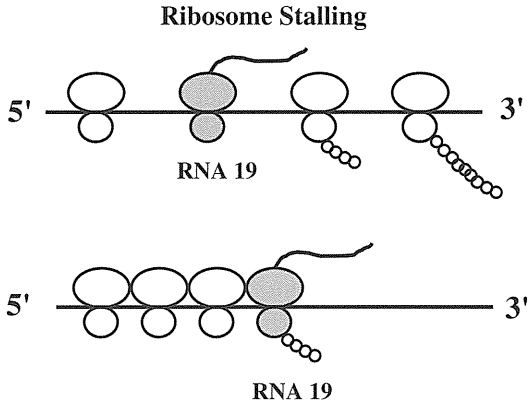

Fig. 4. xRibosomal stalling. The protein synthesis defect has been proposed to be due to stalling of translation by pseudoribosomes that have incorporated RNA 19, an incompletely processed transcript reported to accumulate in A3243 mutant cells, in place of 16 S rRNA, or possibly to defective posttranscriptional modification of the $tRNA^{Leu(UUR)}$ [31].

2.6. Aminoacylation

The decrease in level of total $tRNA^{Leu(UUR)}$ observed in the mutant cell lines (46–62% of the control values) could arise either from decreased rate of formation from the corresponding primary heavy strand transcript or from a decreased metabolic stability [32]. The increased amount of RNA 19, which may be a precursor of $tRNA^{Leu(UUR)}$, was demonstrated in ρ^0 cybrid system as well as somatic tissues in MELAS patients. RNA 19 may suggest the former possibility. On the other hand, the A3243G mutation could perfectly destabilize the tertiary structure of the molecule, and mutant $tRNA^{Leu(UUR)}$ becomes more susceptible to nucleolytic attack [13,33]. It is proposed that mutant tRNA induces the misincorporation of amino acids in mitochondrial DNA encoded polypeptides. However, the demonstration of aminoacylation by mutant tRNA has been little pursued because a chemical amount of the mutant tRNA has not been purified, probably due to technical difficulties. In 2000, Yasukawa succeeded in purifying the mutant $tRNA^{Leu(UUR)}$ molecules in a chemical amount by taking advantage of the solid phase probing method [34], and clearly demonstrated that the mutant $tRNA^{Leu(UUR)}$ is aminoacylated with leucine only. However the extent of aminoacylation of the mutant tRNAs was relatively low. The total amounts of leucyl-$tRNA^{Leu(UUR)}$ with the mutations were estimated to be less than 30% that of the wild-type counterpart [35]. To determine if the decreased fraction of aminoacylated $tRNA^{Leu(UUR)}$ in mutant cells was due to a defect in the ability of mutant tRNA to be aminoacylated by the human mitochondrial leucyl-tRNA synthetase, Park et al. examined the aminoacylation kinetics of wild-type and mutant $tRNA^{Leu(UUR)}$, using both native and in vitro transcribed $tRNA^{Leu(UUR)}$ [36]. An A3243G mutant $tRNA^{Leu(UUR)}$ was 25-fold less efficiently aminoacylated in vitro, compared to the wild-type $tRNA^{Leu(UUR)}$. There are many evidences that aminoacylation capacities in $tRNA^{Leu(UUR)}$ gene mutations are reduced [37]. The reduced amount of aminoacyl-$tRNA^{Leu(UUR)}$ with the A3243G mutation could explain the reduction in protein synthesis.

2.7. Modified defects at wobble position in mitochondrial tRNA gene

A number of reports suggest that a decrease of protein synthesis cannot explain the decline in respiratory enzyme activity or in oxygen consumption [38,39]. Even when the mitochondrial protein synthesis rate was normal, the enzymatic activity of complex I was observed to be significantly affected in cybrid clones containing 60% to 95% mutant mtDNA. The muscle form of Complex I deficiency turned out to be MELAS clinically and was confirmed to have an A3243G mutation in all patients [40]. Thus, the decrease in protein synthesis may not itself contribute directly to the pathogenesis caused by mitochondrial dysfunction. Some unusual mobilities of proteins in SDS-polyacrylamide gel electrophoresis have been reported [18,38], which strongly suggest that amino acids were misincorporated into the proteins synthesized in the mitochondria with the mutant mtDNA. The steady-state amounts of $tRNA^{Leu(UUR)}$ with the A3243G or the T3271C mutation in the respective cybrid clones were about 30% that of the wild-type in the control cybrid clones with wild type mtDNA [35]. In contrast, the steady-state amounts of $tRNA^{Phe}$ and $tRNA^{Ile}$ (encoded upstream and downstream of the $tRNA^{Leu(UUR)}$gene) remained unchanged in both the mutant and control cybrid cells. The life span of the mutant $tRNA^{Leu(UUR)}$ is significantly shortened. The half-life of the wild-type $tRNA^{Leu(UUR)}$ was estimated to be about 56 h, whereas those of the A3243G and T3271C mutants were only about 6 and 12 h. Therefore the reduced steady-state levels were due to the shortened life spans of the mutant tRNAs. Yasukawa found that the wild-type $tRNA^{Leu(UUR)}$ contains an unknown modified uridine at the wobble position and that this modification occurs at the uracil base (Fig. 1B). In contrast, this uridine modification is absent in the $tRNA^{Leu(UUR)}$ with a mutation at either np A3243G or T3271C. It is interesting to note that both of the mutant $tRNA^{Leu(UUR)}$ are deficient in the modification at the wobble position despite having mutations at different positions. Modified defects at wobble position in mitochondrial tRNA gene are also demonstrated by primer extension methods [41]. The deficiency in uridine modification at the wobble position in the mutant $tRNA^{Leu(UUR)}$ strongly suggests mistranslation by these mutant tRNAs according to the mitochondrial wobble rule, which is also demonstrated in other tRNA mutation in MERRF (myoclonus epilepsy with ragged-red fibers) [42–45]. Although mutant $tRNA^{Leu(UUR)}$ does not follow the wobble rule, the mutant $tRNA^{Leu(UUR)}$ is aminoacylated with only leucine, not with other aminoacids. The stability and aminoacylation of the mutant $tRNA^{Leu(UUR)}$ were found to be decreased, suggesting that the molecular pathogenesis of MELAS could be a combination of a lowered availability of aminoacyl $tRNA^{Leu(UUR)}$ and defective translation. This is the first observation of a common modification defect affected by different point mutations within a single tRNA gene.

2.8. Threshold effects in various steps in the cell or in the organs

The phenotypic threshold effect observed at the single-cell level could arise when the products of the wild-type mtDNA can no longer "complement" the effects of the mutated ones [46,47]. For instance, a heteroplasmic mutation in mtDNA will result in the co-existence of mutated mRNAs, mutated tRNAs and defective respiratory chain subunits along with their wild-type homologues. These wild-type molecules may be sufficient to support normal function of the organelle until their levels fall below a critical value (threshold), at which point they can no longer compensate for the effect of the mutation, leading to impairment of mitochondrial function. The phenotypic threshold effect is based on this reserve of different macromolecules (mRNAs, tRNAs, subunits), and can then be considered as a protective mechanism providing a safety margin against the effects of deleterious mutations. Above complementation can occur at different levels of mitochondrial gene expression, such as 1) gene transcription, 2) structural stability of the tRNAs, 3) maturation process of the tRNAs, ribosomal RNA, and mRNAs, 4) wobble modification of tRNAs, 5) aminoacylation, 6) translation, 7) molecular assembly of the active form of enzyme complexes in harmony with mitochondrial and nuclear-encoded polypeptides, 8) locate to the mitochondrial inner membrane, 9) biochemical overall function of mitochondria in the cell, 10) biochemical overall function of mitochondria in the organ, 11) original threshold of organ to the mitochondrial energy requirement. The cells which require high energy states, such as neurons, muscles, heart, and kidneys, may be more severely affected by the threshold level of mutation than cell that require low energy levels. The phenotypes in the severity of the disease may influence various factors listed above and are more complicated to elucidate.

2.8.1. Summary of molecular mechanisms of mitochondrial cytopathy

The mutation creates the protein synthesis defects caused by 1) decreased life span of steady state amount of $tRNA^{Leu(UUR)}$ molecules; 2) decreased ratio of aminoacyl-$tRNA^{Leu(UUR)}$ versus uncharged $tRNA^{Leu(UUR)}$ molecules; 3) accumulation of processing intermediates such as RNA 19, 4) wobble modification defects leading to translation defect. The A3243G mutation shows dominant negative effects in the processing system of mitochondrial transcription seen in both transmitochondrial cell and muscles in MELAS patients. Molecular mechanisms described above may contribute to respiratory chain enzyme defects, especially complex I, and lead to the mitochondrial cytopathy seen in the MELAS patients. Moreover the A3243G mutation affects the nuclear background [46,47], resulting in a high glycolytic rate, increased lactate production, reduced glucose oxidation, impaired NADH-response, reduced mitochondrial membrane potential, markedly reduced ATP production, deranged cell calcium handling with an increased cytosolic calcium handling with an increased cytosolic calcium load, an increased amount of reactive oxygen species in cybrid cells, reduced insulin secretion, premature aging, and deregulation of genes involved in the metabolism of amino groups and urea genesis. The above mechanism may lead to the cytotoxic edema seen in stroke-like episodes in MELAS.

3. Pathophysiology of mitochondrial angiopathy in MELAS

3.1. Hypotheses of stroke-like episodes in MELAS

The primary cause for stroke-like episodes in young MELAS patients—whether 1) mitochondrial cytopathy, 2) mitochondrial angiopathy, 3) non-ischemic neurovascular cellular mechanism, or combined—remains controversial. Mitochondrial cytopathy is caused by an oxidative phosphorylation defect in neurons, glia, or both as supported by evidence of an oxidative phosphorylation defect described by molecular pathogenesis section. Mitochondrial angiopathy is caused by the endothelial dysfunction evidenced by pathological, vascular physiological [11], or therapeutic findings [9,10]. Finally, the non-ischemic neurovascular cellular mechanism has been recently proposed by the clinical and neuroimaging data by Iizuka et al. [3].

3.2. Mitochondrial angiopathy in MELAS

Mitochondrial angiopathy with degenerative changes in small arteries and arterioles in the brain has been reported in autopsy cases of MELAS patients [6,7]. The mitochondria in the endothelium and smooth muscle cells of cerebral arterioles and capillaries also proliferate in a similar fashion as an area of ragged-red fibers (RRFs). Abnormal accumulation of mitochondria in vascular endothelial cells and smooth muscle cells is responsible for the infarct-like lesions [48]. These blood vessels have been designated as strongly succinate dehydrogenase-reactive vessels (SSVs), since they are rich in abnormal mitochondria [8]. Unlike RRFs and SSVs seen in MERRF and Kearns–Sayre syndrome (KSS), RRFs and SSVs seen in MELAS are typically cytochrome c oxidase (COX) positive, while those seen in MERRF or KSS are mostly COX negative, what is known as the "MELAS paradox"[49]. Since nitric oxide (NO) can bind to the active site of COX and displace heme-bound oxygen, hyperactive COX may decrease the regional NO concentration and lead to the segmental vasodilatation defect in SSV regions. Although infarct-like lesions histopathologically and stroke-like episodes clinically may not be caused simply by occlusion or obliteration of small vessels, this mitochondrial angiopathy, which can be severe in pial arterioles and small arteries, seems to explain the distribution of multiple areas of necrosis [50]. Since MELAS was associated with respiratory dysfunction, accumulated superoxide radical anion may react with nitric oxide to create the powerful oxidant hydroxypernitrite which may induce the neuronal apoptosis or cell damage [51]. All findings, described here, suggest that mitochondrial angiopathy is a unique and common change in all MELAS brains examined. This pathological abnormality, called mitochondrial angiopathy, may lead to the vasogenic edema seen in stroke-like episodes in MELAS.

3.3. Non-ischemic neurovascular cellular mechanism

Iizuka et al. proposed that the stroke-like episodes in MELAS may reflect neuronal hyperexcitability (epileptic activity), which increases energy demand and creates an imbalance between energy requirements and the adequate availability of ATP due to an oxidative phosphorylation defect, particularly in the susceptible neuronal population [3,52]. The generalized cytopathic mechanism and non-ischemic neurovascular cellular mechanism reflect the so-called mitochondrial cytopathy theory.

3.4. Neuro-imaging analysis in stroke-like episodes

Unlike thrombotic or embolic stroke usually seen in adult patients, the stroke-like episodes in MELAS are atypical because they affect young people and are often triggered by febrile illnesses, migraine-like headaches, seizure, psychological stress, and dehydration. Many neuro-imaging studies have been reported at different phases of onset from stroke-like episodes in MELAS through the use of computed tomography (CT), magnetic resonance imaging (MRI), magnetic resonance spectroscopy (MRS), single emission computed tomography (SPECT), and positron emission tomography (PET). Calcification of the basal ganglia is frequently observed in MELAS by CT even before starting the stroke-like episodes. MRI scans of acute stroke-like events show an increased signal on T2-weighted or on fluid attenuation inversion recovery (FLAIR). The regions do not conform to the territories of large cerebral arteries but rather affect the cortex and subjacent white matter with sparing of deeper white matter. Acute changes in these regions may fluctuate, migrate, or even disappear during the time course. Cerebral angiograms in MELAS patients have confirmed absence of large-vessel pathology by demonstrating normal results, increased size of caliber arteries, veins, or capillary blush with early venous filling, with the exception of several case reports [53,54]. MRS studied revealed that the decrease in N-acetylaspartate (NAA), which is thought to be an amino acid specific to neurons, and an increase of lactate, which is reflected of anaerobic metabolism by ^{1}H-magnetic resonance spectroscopy (^{1}H-MRS), were in evidence in the affected areas at acute stroke-like episodes. Kubota et al. reported that L-arginine infusion protect the accumulation of lactate by MRS analysis in stroke-like episodes in MELAS [55]. The increased level of lactate on ^{1}H-MRS is also recognized even in normal appearing regions [56]. Phosphorus MRS studies have shown decreased levels of high-energy phosphate compounds in the brains of MELAS patients [57], showing that mitochondrial cytopathy constantly exists in the MELAS patient. SPECT studies have generally revealed that the increased tracer accumulation was reported in acute (several days) and subacute stage (month) from the onset of stroke-like episodes and lasted for several months. In the chronic stage (several months or years later), the decreased tracer accumulation was reported. However, in the hyperacute stage (3 h after the onset of stroke-like episodes), we observed hypoperfusion by SPM-SPECT analysis [58]. Moreover, the hypoperfusion and the hyperperfusion areas are both demonstrated in the MELAS patients not only at an acute phase but at an interictal phase, showing that MELAS has inappropriate cerebral circulation [54]. Moreover, MELAS showed hypoperfusion in the posterior cingulated cortex by SPM-SPECT, which is the common finding in Alzheimer disease, and may be related to the dementia state usually seen in the progressive stage of MELAS. There are several PET studies using ($rCMRO_2$), [^{62}Cu]-diacetyl bis (N4-methylthiosemicarbazone) (^{62}Cu-ATSM), and [^{18}F]-fluorodeoxyglucose (^{18}FDG) in stroke-like regions [59,60]. All of the PET studies of

patients have revealed decreased oxygen consumption relative to glucose utilization, further confirming the impairment of oxidative phosphorylation [61]. The dissociation in PET findings between cerebral glucose and oxygen metabolism may be the characteristic feature of MELAS, suggesting the mitochondrial cytopathy theory or non-ischemic neurovascular cellular mechanism. Diffusion-weighted (DWI) imaging is a new MRI technique for detecting diffusion of water molecules. Using DWI, local water mobility can be assayed as the absolute value of tissue water and expressed as the apparent diffusion coefficient (ADC). It has been shown using a stroke model in rats that ADC (a marker for cytotoxic brain edema) significantly declined within the first 5–10 min after stroke onset, while T2-relaxation time (a marker for vasogenic brain edema) increased as early as at the first T2-imaging time-point (20–35 min after embolization) [62]. The acute phase of stroke-like lesions in MELAS appear as a high signal on DWI with normal or increased ADC values, suggesting vasogenic edema which support the mitochondrial angiopathy theory [63,64]. On the contrary, many case reports found a decrease in ADC, which suggests mitochondrial cytopathy theory [65]. Recently, it was reported that increased and decreased ADC portions are mixed in stroke-like lesions, in which the increased ADC portion showed disappearance of the lesions thereafter, and the decreased portion showed persistent lesions. They suggested that there might be different levels of mitochondrial energetic transport impairment, correlated with cellular dysfunction. Specifically, this would be a mild energy failure resulting in moderate cellular dysfunction, responsible for vasogenic edema (high ADCs) and a severe energy failure resulting in irreversible cellular failure with cytotoxic edema (low ADCs) [66].

3.5. Endothelial dysfunction in MELAS

Physiologically, MELAS patients have a decreased vasodilation capacity in small arteries examined by flow mediated vasodilatation (FMD) methods, sized from 3 to 5 mm in their diameter [11]. MELAS patients have significantly decreased levels of L-arginine at acute phase of stroke-like episodes, which plays an important role in endothelial-dependent vascular relaxation [67], vasodilatation may be more severely affected in MELAS. Since MELAS patients have defective respiratory chain enzyme activities, a high NADH/NAD + ratio inhibits the NO synthetase reaction to cause a decreased production of NO at the endothelial cells or smooth muscle cells in the artery. In addition, ADMA (asymmetrical dimetyl-arginine), a risk factor of ischemic heart disorders, was relatively increased in MELAS patients [10], which may lead to a negative effect on the endothelial NO synthetase activity. If hyperactive COX may decrease the regional NO concentration as described in "MELAS paradox" [49], all of the above scenarios lead to the segmental vasodilatation defect especially in the segment of SSV regions in the cerebral artery or arterioles. The investigator-mediated clinical trial of L-arginine on MELAS (Dr. Koga as a principle investigator) to cure the symptoms of stroke-like episodes at acute phase, and to prevent or decrease the severity of stroke-like episodes at interictal phase of MELAS are on-going at 15 institutions of university hospital in Japan.

3.5.1. Summary of mitochondrial angiopathy and L-arginine effects

Pathophysiological mechanisms of mitochondrial angiopathy and the effects of L-arginine are summarized in Fig. 5.

4. Conclusion and future direction

The possible pathogenic mechanism of stroke-like episodes in MELAS may not be simple but complicated as described by the mechanisms in mitochondrial cytopathy and in mitochondrial angiopathy. Mitochondrial cytopathy has been demonstrated clearly as molecular and cellular defects by trans-mitochondrial cellular models. Mitochondrial angiopathy also has been demonstrated in brain and muscle pathology and vascular physiology. Although the results of

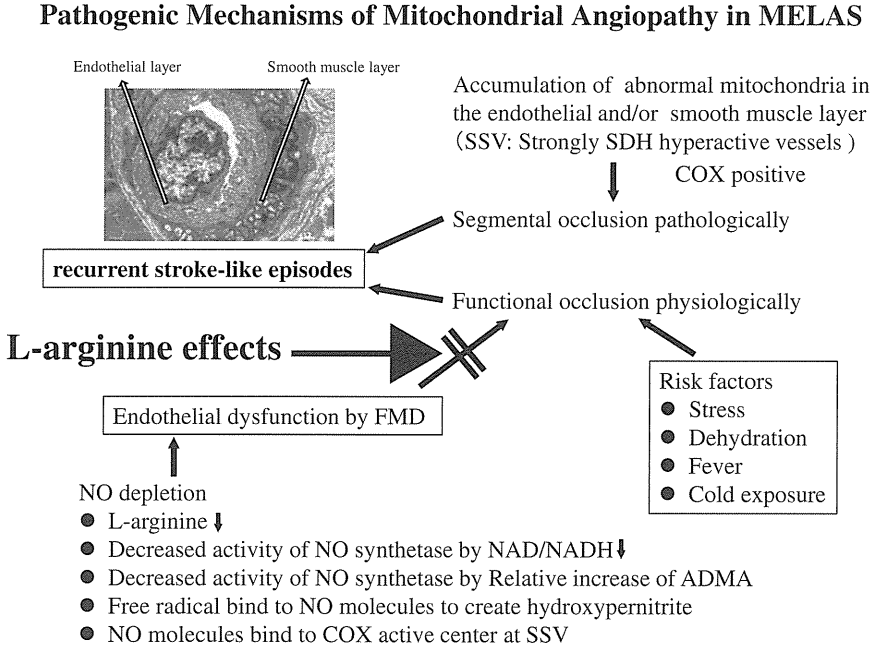

Fig. 5. Pathogenic mechanisms of mitochondrial angiopathy in MELAS. Segmental occlusions of small artery or arteriolen are evident in brain as well as in muscle pathology, in which abnormal accumulations of mitochondria have seen in endothelial and smooth muscle layers [6,7]. This phenomenon is recognized as SSVs in muscle and brain in MELAS [8], whereby mitochondrial function is more profoundly defective than the rest of the vessels, and demonstrated as endothelial dysfunction by FMD physiologically [11]. In MELAS patients, decreased levels of L-arginine is reported at acute phase of stroke-like episodes, a potent donor of NO, is also responsible for NO-dependent vascular dilatation defect. The decreased NAD/NADH ratio and accumulation of superoxide come from respiratory chain deficiency results in the inhibition of NO synthetase at generation process and decrease NO molecules by binding to create hydroxypernitrite, also contribute to the NO-dependent vasodilation abnormality. Since SSVs has usually high COX-positive feature histochemically, high COX activity decrease the residual NO molecules by binding to COX reactive center. The mental stress, dehydration, fever and cold exposure are also very important factors to increase the risk of the stroke-like episodes in MELAS.

neuro-imaging studies are controversial and are difficult to evaluate, there are several specific findings which may lead to the pathophysiology of stroke-like episodes in MELAS. We have to elucidate what is the trigger of stroke-like episodes in MELAS in future. Currently L-arginine therapy, to cure the symptoms of stroke-like episodes at acute phase, and to prevent or decrease the severity of stroke-like episodes at interictal phase of MELAS, is the most promising therapy for this incurable disorder. Global clinical trial of L-arginine on MELAS using randomized double blind placebo control protocol may be done in the nearer future.

References

[1] S.G. Pavlakis, P.C. Phillips, S. DiMauro, D.C. De Vivo, L.P. Rowland, Ann. Neurol. 16 (1984) 481–488.
[2] S. DiMauro and M. Hirano. MELAS, R.A. Pagon, T.C. Bird, C.R. Dolan, K. Stephens and editors, Seattle (WA), University of Washington Seattle, *Gene reviews* [Internet;http://www.ncbi.nlm.nih.gov/books/NBK1233/] (1993) updated 2010 Oct 14
[3] T. Iizuka, F. Sakai, Future Neurol. 5 (2010) 61–83.
[4] Y. Goto, I. Nonaka, A. Horai, Nature 348 (1990) 651–653.
[5] Y. Goto, S. Horai, T. Matsuoka, Y. Koga, K. Nihei, M. Kobayashi, I. Nonaka, Neurology 42 (1992) 545–550.
[6] E. Ohama, S. Ohara, F. Ikuta, K. Tanaka, M. Nishizawa, T. Miyatake, Acta Neuropathol. 74 (1987) 226–233.
[7] M. Kishi, Y. Yamamura, T. Kurihara, N. Fukuhara, K. Tsuruta, S. Matsukura, T. Hayashi, M. Nakagawa, M. Kuriyama, J. Neurol. Sci. 86 (1988) 31–40.
[8] H. Hasegawa, T. Matsuoka, Y. Goto, I. Nonaka, Ann. Neurol. 29 (1991) 601–605.
[9] Y. Koga, M. Ishibashi, I. Ueki, S. Yatsuga, R. Fukiyama, Y. Akita, T. Matsuishi, Neurology 58 (2002) 827–828.
[10] Y. Koga, Y. Akita, J. Nishioka, S. Yatsuga, N. Povalko, Y. Tanabe, S. Fujimoto, T. Matsuishi, Neurology 64 (2005) 710–712.
[11] Y. Koga, Y. Akita, N. Junko, S. Yatsuga, N. Povalko, R. Fukiyama, M. Ishii, T. Matsuishi, Neurology 66 (2006) 1766–1769.
[12] J.P. Goddard, Prog. Biophys. Mol. Biol. 32 (1977) 233–308.
[13] M.D. Roy, L.M. Wittenhagen, S.O. Kelley, RNA 11 (2005) 254–260.
[14] J. Finsterer, Acta Neurol. Scand. 116 (2007) 1–14.
[15] B. Sohm, M. Frugier, H. Brule, K. Olszak, A. Przykorska, C. Florentz, J. Mol. Biol. 328 (2003) 995–1010.
[16] M.P. King, G. Attardi, Cell 52 (1998) 811–819.
[17] M.P. King, G. Attardi, Science 246 (1989) 500–503.
[18] A. Chomyn, A. Martinuzzi, M. Yoneda, A. Daga, O. Hurko, D. Johns, S.T. Lai, I. Nonaka, S. Angelini, G. Attardi, Proc. Natl. Acad. Sci. U. S. A. 89 (1992) 4221–4225.
[19] M.P. King, Y. Koga, M. Davidson, E.A. Schon, Mol. Cell. Biol. 12 (1992) 480–490.
[20] R. Gelfand, G. Attardi, Mol. Cell. Biol. 1 (1981) 497–511.
[21] J. Montoya, G.L. Gaines, G. Attardi, Cell 34 (1983) 151–159.
[22] B. Kruse, N. Narasimhan, G. Attardi, Cell 58 (1989) 391–397.
[23] J.F. Hess, M.A. Parisi, J.L. Bennett, D.A. Clayton, Nature 351 (1991) 236–239.
[24] Y. Koga, M. Davidson, E.A. Schon, M.P. King, Nucleic Acids Res. 21 (1993) 657–662.
[25] L. Levinger, I. Oestreich, C. Florentz, M. Morl, J. Mol. Biol. 337 (2004) 535–544.
[26] P. Kaufmann, Y. Koga, S. Shanske, M. Hirano, S. DiMauro, M.P. King, E.A. Schon, Ann. Neurol. 40 (1996) 172–180.
[27] L.A. Bindoff, N. Howell, J. Poulton, D.A. McCullough, K.J. Morten, R.N. Lightowlers, D.M. Turnbull, K. Weber, J. Biol. Chem. 268 (1993) 19559–19564.
[28] Y. Koga, M. Yoshino, H. Kato, Ann. Neurol. 43 (1998) 835.
[29] Y. Koga, M. Davidson, E.A. Schon EA, M.P. King, Muscle Nerve 3 (1995) S119–S123 suppl.
[30] A. Koga, Y. Koga, Y. Akita, M. Yoshino, H. Kato, Neuromuscul. Disord. 13 (2003) 259–262.
[31] E.A. Schon, Y. Koga, M. Davidson, C.T. Moraes, M.P. King, Biochem. Biophys. Acta 1101 (1992) 206–209.
[32] A. Chomyn, J.A. Enriquez, V. Micol, P. Fernandez-Silva, G. Attardi, J. Biol. Chem. 275 (2000) 19198–19209.
[33] M. Helm, C. Florentz, A. Chomyn, G. Attardi, Nucleic Acids Res. 27 (1999) 756–763.
[34] K. Wakita, Y. Watanabe, T. Yokogawa, Y. Kumazawa, S. Nakamura, T. Ueda, K. Watanabe, K. Nishikawa, Nucleic Acids Res. 22 (1994) 347–353.
[35] T. Yasukawa, T. Suzuki, T. Suzuki, T. Ueda, S. Ohta, K. Watanabe, J. Biol. Chem. 275 (2000) 4251–4257.
[36] H. Park, M. Davidson, M.P. King, Biochemistry 42 (2003) 958–964.
[37] R. Hao, Y.N. Yao, Y.G. Zheng, M.G. Xu, E.D. Wang, FEBS Lett. 578 (2004) 135–139.
[38] D.R. Dunbar, P.A. Moonie, M. Zeviani, J. Holt, Hum. Mol. Genet. 5 (1996) 123–129.
[39] H. Flierl, P. Reichmann, J. Seibel, Biol. Chem. 272 (1997) 27189–27196.
[40] Y. Koga, I. Nonaka, M. Kobayashi, M. Tojyo, K. Nihei, Ann. Neurol. 24 (1988) 749–756.
[41] Y. Kirino, T. Yasukawa, S. Ohta, S. Akira, K. Ishihara, K. Watanabe, T. Suzuki, Proc. Natl. Acad. Sci. U. S. A. 101 (2004) 15070–15075.
[42] T. Yasukawa, T. Suzuki, N. Ishii, S. Ohta, K. Watanabe, EMBO J. 20 (2001) 4794–4802.
[43] T. Yasukawa, T. Suzuki, N. Ishii, T. Ueda, S. Ohta, K. Watanabe, FEBS Lett. 467 (2000) 175–178.
[44] Y. Kirino, T. Yasukawa, S.K. Marjavaara, H.T. Jacobs, I.J. Holt, K. Watanabe, T. Suzuki, Hum. Mol. Genet. 15 (2006) 897–904.
[45] T. Suzuki, T. Suzuki, T. Wada, K. Saigo, K. Watanabe, EMBO J. 21 (2002) 6581–6589.
[46] R. Rossignol, M. Malgat, J.P. Mazat, T. Letellier, J. Biol. Chem. 274 (1999) 33426–33432.
[47] R. Rossignol, B. Faustin, C. Rocher, M. Malgat, J.P. Mazat, T. Letellier, Biochem. J. 370 (2003) 751–762.
[48] R. Sakuta, I. Nonaka, Ann. Neurol. 25 (1989) 594–601.
[49] A. Naini, P. Kaufmann, S. Shanske, K. Engelstad, D.C. De Vivo, E.A. Schon, J. Neurol. Sci. 229–230 (2005) 187–193.
[50] C. Tanahashi, A. Nakayama, M. Yoshida, M. Ito, N. Mori, Y. Hashizume, Acta Neuropathol. 99 (2000) 31–38.
[51] M.A. Moro, A. Almeida, J.P. Bolanos, I. Lizasoain, Free Radical Biology & Medicine 39 (2005) 1291–1304.
[52] T. Iizuka, F. Sakai, T. Ide, S. Miyakawa, M. Sato, S. Yoshii, J. Neurol. Sci. 257 (2007) 126–138.
[53] A. Noguchi, Y. Shoji, M. Matsumori, K. Komatsu, G. Takada, Pediatr. Neurol. 33 (2005) 70–71.
[54] T. Iizuka, Y. Goto, S. Miyakawa, M. Sato, Z. Wang, K. Suzuki, J. Hamada, A. Kurata, F. Sakai, J. Neurol. Sci. 278 (2009) 35–40.
[55] M. Kubota, Y. Sakakihara, M. Mori, T. Yamagata, M. Momoi-Yoshida, Brain Dev. 26 (2004) 481–483.
[56] E. Wilichowski, P.J. Pouwels, J. Frahm, F. Hanefeld, Neuropediatrics 30 (1999) 256–263.
[57] P. Kaufmann, D.C. Shungu, M.C. Sano, S. Jhung, K. Engelstad, E. Mitsis, X. Mao, S. Shanske, M. Hirano, S. DiMauro, D.C. De Vivo, Neurology 62 (2004) 1297–1302.
[58] J. Nishioka, Y. Akita, S. Yatsuga, K. Katayama, T. Matsuishi, M. Ishibashi, Y. Koga, Brain Dev. 30 (2008) 100–105.
[59] M. Ikawa, H. Okazawa, K. Arakawa, T. Kudo, H. Kimura, Y. Fujibayashi, M. Kuriyama, M. Yoneda, Mitochondrion 9 (2009) 144–148.
[60] T. Nariai, K. Ohno, Y. Ohta, K. Hirakawa, K. Ishii, M. Senda, J. Neuroimaging 11 (2001) 325–329.
[61] M.J. Molnár, A. Valikovics, S. Molnár, L. Trón, P. Diószeghy, F. Mechler, B. Gulyás, Neurology 55 (2000) 544–548.
[62] T. Gerriets, E. Stolz, M. Walberer, C. Müller, A. Kluge, M. Kaps, M. Fisher, G. Bachmann, Brain Res. Protoc. 12 (2004) 137–143.
[63] T. Ohshita, M. Oka, Y. Imon, C. Watanabe, S. Katayama, S. Yamaguchi, T. Kajima, Y. Mimori, S. Nakamura, Neuroradiology 42 (2000) 651–656.
[64] H. Ito, K. Mori, M. Harada, M. Minato, E. Naito, M. Takeuchi, Y. Kuroda, S. Kagami, Brain Dev. 30 (2008) 483–488.
[65] X.Y. Wang, K. Noguchi, S. Takashima, N. Hayashi, S. Ogawa, H. Seto, Neuroradiology 45 (2003) 640–643.
[66] S. Stoquart-Elsankari, P. Lehmann, B. Périn, C. Gondry-Jouet, O. Godefroy, J. Neurol. 255 (2008) 1593–1595.
[67] X.L. Wang, A.S. Sim, R.F. Badenhop, R.M. McCredie, D.E. Wilcken, Nat. Med. 2 (1996) 41–45.

Biochimica et Biophysica Acta 1820 (2012) 619–624

Contents lists available at ScienceDirect

Biochimica et Biophysica Acta

journal homepage: www.elsevier.com/locate/bbagen

MELAS: A nationwide prospective cohort study of 96 patients in Japan ☆

Shuichi Yatsuga [a,d], Nataliya Povalko [a], Junko Nishioka [a], Koju Katayama [a], Noriko Kakimoto [a], Toyojiro Matsuishi [a], Tatsuyuki Kakuma [b], Yasutoshi Koga [a,*] and Taro Matsuoka for MELAS Study Group in Japan [c]

[a] Department of Pediatrics and Child Health, Kurume University Graduate School of Medicine, Kurume, Japan
[b] Department of Biostatistics, Kurume University Graduate School of Medicine, Kurume, Japan
[c] MELAS study group in Japan
[d] Research Program of Molecular Neurology, Biomedicum Helsinki, University of Helsinki, Helsinki, Finland

ARTICLE INFO

Article history:
Received 30 January 2011
Accepted 21 March 2011
Available online 2 April 2011

Keywords:
Prevalence
MELAS
Cohort study
Natural course
Survival curve
Severity of disease

ABSTRACT

Background: MELAS (mitochondrial myopathy, encephalopathy, lactic acidosis and stroke-like episodes) (OMIM 540000) is the most dominant subtype of mitochondrial myopathy. The aim of this study was to determine the prevalence, natural course, and severity of MELAS.
Methods: A prospective cohort study of 96 Japanese patients with MELAS was followed between June 2003 and April 2008. Patients with MELAS were identified and enrolled based on questionnaires administered to neurologists in Japan. MELAS was defined using the Japanese diagnostic criteria for MELAS. Two follow-up questionnaires were administered to neurologists managing MELAS patients at an interval of 5 years.
Results: A prevalence of at least 0.58 (95% confidential interval (CI), 0.54–0.62)/100,000 was calculated for mitochondrial myopathy, whereas the prevalence of MELAS was 0.18 (95%CI, 0.02–0.34)/100,000 in the total population. MELAS patients were divided into two sub-groups: juvenile form and adult form. Stroke-like episodes, seizure and headache were the most frequent symptoms seen in both forms of MELAS. Short stature was significantly more frequent in the juvenile form, whereas hearing loss, cortical blindness and diabetes mellitus were significantly more frequent in the adult form. According to the Japanese mitochondrial disease rating scale, MELAS patients showed rapidly increasing scores (mean ± standard deviation, 12.8 ± 8.7) within 5 years from onset of the disease. According to a Kaplan–Meier analysis, the juvenile form was associated with a higher risk of death than the adult form (hazard ratio, 3.29; 95%CI, 1.32–8.20; $p = 0.0105$).
Conclusions and General Significance: We confirmed that MELAS shows a rapid degenerative progression within a 5-year interval and that this occurs in both the juvenile and the adult forms of MELAS and follows different natural courses. This article is part of a Special Issue entitled: Biochemistry of Mitochondria.

1. Introduction

Mitochondrial dysfunction increases the risk of developing various human diseases, including degenerative neuromuscular disorders, diabetic or metabolic conditions, and cancer; it also affects the aging process [1]. The classical clinical entity in this category is the so-called mitochondrial myopathy, in which mitochondrial dysfunction is caused by mitochondrial or nuclear genetic abnormalities. The disease, which encompasses mitochondrial myopathy, encephalopathy, lactic acidosis and stroke-like episodes (MELAS) (OMIM 540000), is characterized by the early onset of stroke-like episodes and was first described by Pavlakis and colleagues in 1984 [2]; it is thought to be the most dominant subtype of mitochondrial dysfunction. At least 39 distinct mitochondrial DNA mutations have been associated with MELAS [3]; however, approximately 80% of MELAS patients have an A3243G mutation in the mitochondrial $tRNA^{Leu(UUR)}$ gene (OMIM 590050) [4] and [5]. Because this mutation was also found to be a major genetic abnormality in diabetes mellitus, it may be a particularly common genetic variant in human populations [6]. Although more than 26 years have passed since the clinical and pathological definition of MELAS, there are few reports on its prevalence and epidemiology, and no reports exist on the natural course, survival rate or severity of the disease in a cohort study, meta-analysis, or nationwide survey [7] and [8]. In this study, we determined the prevalence, clinical symptoms, natural course, severity, and survival rate of MELAS patients in a nationwide Japanese

Abbreviations: JMDRS, Japanese mitochondrial disease rating scale; NPMDS, Newcastle pediatric mitochondrial disease scale; NMDAS, Newcastle mitochondrial disease adult scale

☆ This article is part of a Special Issue entitled: Biochemistry of Mitochondria.

* Corresponding author. Department of Pediatrics and Child Health, Kurume University School of Medicine, 67 Asahi-Machi, Kurume City, Fukuoka 30-0011, Japan. Tel.: +81 942 31 7565; fax: +81 942 38 1792.
E-mail address: yasukoga@med.kurume-u.ac.jp (Y. Koga).

0304-4165/$ – see front matter © 2011 Elsevier B.V. All rights reserved.
doi:10.1016/j.bbagen.2011.03.015

cohort study. Additionally, we also evaluated the clinical rating scale that may be a very useful tool for the assessment of efficacy of therapeutic approach for mitochondrial myopathy.

2. Materials and methods

2.1. Study design, patients, and data collection for the Japanese cohort study

The cohort study was performed using questionnaires. To determine the prevalence of mitochondrial myopathies throughout the country, the first questionnaire was mailed in 2001 to 2236 neurology departments within Japan (1474 departments with pediatric neurologists and 762 departments with adult neurologists, including governmental, public, private and university hospitals with 50 beds or more). Patients' medical records were evaluated using MELAS diagnostic criteria (Table 1) and adequately screened. In 2003, after compiling the results of the first questionnaire, we mailed a second questionnaire to the neurologists who had examined MELAS patients in 2001. In 2008, we mailed a third questionnaire to the same group of neurologists. The second and third questionnaires included a Japanese mitochondrial disease rating scale (JMDRS) (Supplemental Table 1). Relevant information from the medical records of eligible patients was transcribed onto case report forms by neurologists, who were later interviewed by telephone if ambiguous data or unsatisfactory descriptions were found in the case report forms. Detailed documentation of the patients' clinical status was compiled by the same neurologists. The case report form was originally constructed according to the JMDRS and was updated whenever the scores were altered. Written informed consent was obtained from the patients or their legal guardians. The study protocol was approved by the Institutional Review Board (Kurume University #9715).

2.2. Diagnostic criteria for MELAS

The nationwide survey of MELAS in this study is based on the definitive diagnosis of MELAS presented in Table 1.

Table 1
Diagnostic criteria for MELAS (MELAS study committee in Japan).

Category A. Clinical findings of stroke-like episodes
1. Headache with vomiting
2. Seizure
3. Hemiplegia
4. Cortical blindness or hemianopsia
5. Acute focal lesion observed via brain imaging[a]

Category B. Evidence of mitochondrial dysfunction
1. High lactate levels in plasma and/or cerebral spinal fluid or deficiency of mitochondrial-related enzyme activities[b]
2. Mitochondrial abnormalities in muscle biopsy[c]
3. Definitive gene mutation related to MELAS[d]

Definitive MELAS
Two items of Category A and two items of Category B (four items or more)

Suspicion of MELAS
One item of Category A and two items of Category B (at least three items)

[a] Focal brain abnormalities in CT and/or MRI.

[b] 2 mmol/L (18mg/dl) or more lactate in plasma at rest or in cerebral spinal fluid and/or deficiency of electron transport chain enzyme, pyruvate-related, TCA cycle-related enzymes or lipid metabolism-related enzymes in somatic cells (desirable for muscle cells).

[c] RRF (ragged-red fiber) in modified Gomori's trichrome stain and/or SSV (strongly SDH-reactive blood vessels) in succinate dehydrogenase stain, cytochrome *c* oxidase-deficient fibers or abnormal mitochondria in electron microscopy.

[d] Definitive mitochondrial gene mutations reported in the literature (G583A, G1642A, G1644A, A3243G, A3243T, A3252G, C3256T, A3260G, T3271C, T3291C, G3481A, G3697A, T3949C, G4332A, G5521A, A5814G, G7023A, T7512C, A8296G, T8316C, T9957C, A12299C, A12770G, G13042A, A13084T, G13513A, A13514G, A13528G, and G14453A) as of 2010 [3].

2.3. Japanese Mitochondrial Disease Rating Scale (JMDRS)

We prospectively analyzed the clinical progress of MELAS using the JMDRS (Supplementary Table 1), which was revised following the European NeuroMuscular Conference (ENMC) in 2003 [9]. The second and the third questionnaires were also based on the JMDRS and enabled longitudinal analysis of disease progression. We established a rating score for each patient in 2003 and 2008, and these values were used to analyze the clinical severity of MELAS.

2.4. Statistical analysis

Demographic and clinical data for the juvenile and adult forms of MELAS were summarized using descriptive statistics. An unpaired *t*-test was used to test for any differences in the death rates of juvenile and adult forms. Differences between the juvenile and adult forms in the symptoms at onset and throughout the entire follow-up period were evaluated by chi-square tests or Fisher's exacts test when the criteria for the chi-square test were not fulfilled. Alterations in the JMDRS scores between 2003 and 2008 were evaluated using unpaired *t*-tests alone or combined with a Welch correction when variances were significantly different. Survival rates were compared between juvenile and adult forms using the log-rank test. Statistical analyses were performed with the SPSS 11.0 J software package for Windows. $p<0.05$ was considered statistically significant.

3. Results

3.1. Questionnaire responses from the Japanese cohort

We received 1051 responses to the first questionnaire (total 47.0% response rate, 1051/2236); among them, 756 were from pediatric neurology departments(51.3% of responses) and 295 were from adult neurology departments(38.7% of responses). We identified 741 patients with mitochondrial myopathies and of these, 233 were MELAS patients (31.4% of total mitochondrial myopathy patients, 233/741), as described by 105 pediatric neurologists and 29 adult neurologists. We received 64 responses to the second questionnaire (total 47.8% response rate, 64/134): 36 from pediatric neurologists (34.3% response rate, 36/105) and 28 from adult neurologists (96.6% response rate, 28/29). We received 64 responses to the third questionnaire (100% response rate, 64/64); only 96 MELAS patients completed the 5-year cohort study.

3.2. Prevalence of MELAS in Japan

We found 741 cases of mitochondrial myopathy in our cohort study. Based on the MELAS diagnostic criteria (Table 1), we found 233 MELAS patients (juvenile/adult = 111/122) among the Japanese population of approximately 127,434,000 (approximately 22,275,000 under 18 years of age and approximately 105,159,000 over 18 years of age, adult form, according to census data from 2001). The prevalence of mitochondrial myopathy in Japan is therefore at least 0.58 (95% confidence interval (CI), 0.54–0.62)/100,000 in the total population. The prevalence of MELAS is at least 0.18 (95%CI, 0.17–0.19)/100,000 in the total population, 0.50 (95%CI, 0.41–0.59)/100,000 in children under 18 years of age, and 0.12 (95%CI, 0.10–0.14)/100,000 in the population over 18 years of age.

3.3. Demographic and pathological findings of MELAS in the cohort study

Our cohort study included 96 MELAS patients who were followed prospectively for 5 years. A histogram and a density plot showing the various ages of onset in MELAS in these patients indicate an approximately bimodal distribution (Fig. 1). We therefore divided the MELAS patients into two sub-groups to determine whether MELAS

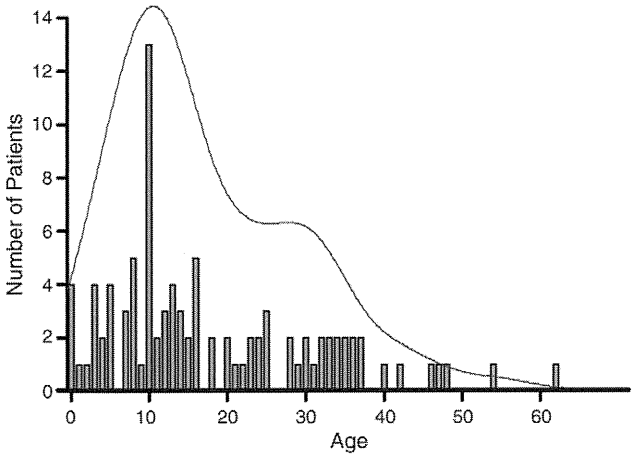

Fig. 1. Histogram detailing age of onset. A histogram and density plot of the various ages of MELAS onset is shown. In total, 96 Japanese patients were identified as having definitive MELAS as determined by diagnostic criteria (Table 1). Given the approximately bimodal distribution of patient age, MELAS patients were divided into two subgroups by the age of onset. Patients with an age of onset less than 18 years old were defined as having the juvenile form of MELAS, and patients with an age of onset greater than 18 years old were defined as having the adult form of MELAS.

has different features depending on the age of onset. Patients with an age of onset under 18 years were defined as having the juvenile form of MELAS, whereas patients with an age of onset above 18 years were defined as having the adult form of MELAS. A summary of the indexed MELAS patients is shown (Table 2). The ages of onset, diagnosis, and death were determined for both juvenile and adult forms. During this study, 17 of the 20 deceased MELAS patients presented with the juvenile form. Causes of death were cardiac insufficiency (7), severe respiratory infection (6), multiple organ insufficiency (3), and unknown causes (4).

Seventy-eight patients received muscle biopsies and 71 patients (91.0%) showed positive findings, including ragged-red fibers (RRF), SDH strongly reactive blood vessels (SSV), or both. However, seven patients presented normal features in the muscle biopsy.

3.4. Symptoms at onset and during the entire course

We evaluated the symptoms at onset in 96 MELAS patients (Table 3). The first sign of any symptoms or events such as seizure, stroke-like episode, or severe headache, which were associated with a neuroimaging-abnormality, was defined as the onset of MELAS. Symptoms at onset and during the entire course were similar as follows; seizure, stroke-like episode, and headache were the most frequent symptoms. Short stature and failure to thrive were significantly more prevalent in the juvenile form than in the adult form. However, hearing loss, diabetes mellitus and hemiplegia were significantly more frequent in the adult form than in the juvenile form.

Table 2
Demographic findings for MELAS cases.

	All form	Juvenile form	Adult
Patient[b] (male/female)	96 (52/44)	58 (35/23)	38 (17/21)
Age of onset, years[a]	17.7 ± 13.6	9.0 ± 4.7	32.2 ± 10.0
Age of diagnosis, years[a]	19.9 ± 13.5	11.0 ± 5.0	33.6 ± 10.6
Age of death, years[a]	18.8 ± 11.5	15.0 ± 7.9	40.0 ± 3.6
Death (%)[b,c]	20 (20.8 %)	17 (29.3 %)	3 (7.9 %)
Time from diagnosis to death[a]	7.3 ± 5.0	6.4 ± 4.5	10.2 ± 8.3
Positive family history[b] (%)	23 (24.0)	13 (22.4)	10 (26.3)
Muscle biopsy examination[b]	78	42	36
Positive findings[b] (%)	71 (91.0)	36 (85.7)	35 (97.2)
RRF[b]	56	24	32
SSV[b]	2	2	0
RRF + SSV[b]	13	10	3
A3243G mutation positive[b] (%)	75 (78.1)	46 (79.3)	29 (76.3)
Other mutation found in mtDNA[b]	4	4	0
Mutation not found[b]	17	8	9

[a] Mean ± SD.
[b] Number.
[c] Death ratio was higher for the juvenile form than for the adult form ($p = 0.0115$).

Table 3
Symptoms.

	Total (%) ($n = 96$)	Juvenile (%) ($n = 58$)	Adult (%) ($n = 38$)
Symptoms at onset			
Seizure	54/96 (56.3)	36/58 (62.1)	18/38 (47.4)
Stroke-like episode	53/96 (55.2)	29/58 (50.0)	24/38 (63.2)
Headache	48/96 (50.0)	27/58 (46.6)	21/38 (55.3)
Short stature[a]	46/96 (47.9)	35/58 (60.3)	11/38 (28.9)
Muscle weakness	36/96 (37.5)	26/58 (44.8)	10/38 (26.3)
General fatigue	30/96 (31.3)	20/58 (34.5)	10/38 (26.3)
Cortical blindness	26/96 (27.1)	15/58 (25.9)	11/38 (28.9)
Failure to thrive[a]	25/96 (26.0)	23/58 (39.7)	2/38 (5.3)
Vomiting/nausea	23/96 (24.0)	17/58 (29.3)	6/38 (15.8)
Hearing loss[a]	21/96 (21.9)	6/58 (10.3)	15/38 (39.5)
Unconsciousness	19/96 (19.8)	10/58 (17.2)	9/38 (23.7)
Teichopsia	18/96 (18.8)	12/58 (20.7)	6/38 (15.8)
Diabetes mellitus[a]	12/96 (12.5)	2/58 (3.4)	10/38 (26.3)
Symptoms in the entire course			
Stroke-like episode	81/96 (84.4)	49/58 (84.5)	32/38 (84.2)
Seizure	68/96 (70.8)	42/58 (72.4)	26/38 (68.4)
Short stature[a]	53/96 (55.2)	37/58 (63.8)	16/38 (42.1)
Headache	52/96 (54.2)	30/58 (51.7)	22/38 (57.9)
Cortical blindness[a]	43/96 (44.8)	21/58 (36.2)	22/38 (57.9)
Muscle weakness	40/96 (41.7)	27/58 (46.6)	13/38 (34.2)
General fatigue	38/96 (39.6)	26/58 (44.8)	12/38 (31.6)
Mental regression	38/96 (39.6)	20/58 (34.5)	18/38 (47.4)
Gait disturbance	37/96 (38.5)	23/58 (39.7)	14/38 (36.8)
Unconsciousness	36/96 (37.5)	20/58 (34.5)	16/38 (42.1)
Teichopsia	31/96 (32.3)	20/58 (34.5)	11/38 (28.9)
Cardiac dysfunction	29/96 (30.2)	18/58 (31.0)	11/38 (28.9)
Failure to thrive[a]	27/96 (28.1)	24/58 (41.4)	3/38 (7.9)
Speech disturbance	22/96 (22.9)	16/58 (27.6)	6/38 (15.8)
Memory loss	20/96 (20.8)	12/58 (20.7)	8/38 (21.1)
Diabetes mellitus[a]	20/96 (20.8)	5/58 (8.6)	15/38 (39.5)

[a] Significant difference between juvenile and adult forms. $p<0.05$ was considered statistically significant. At onset: short stature ($p = 0.0026$), failure to thrive ($p = 0.0001$), hearing loss ($p = 0.0007$), diabetes mellitus ($p = 0.0014$). During follow-up: short stature ($p = 0.0366$), hearing loss ($p = 0.0012$), cortical blindness ($p = 0.0366$), failure to thrive ($p = 0.0004$), diabetes mellitus ($p = 0.0006$).

3.5. Disease progression monitored with the JMDRS

MELAS was monitored in 2003 and 2008 with the JMDRS, which covers (1) activities of daily living, (2) motor functions, (3) special sensory functions, (4) endocrine functions, (5) cardiac functions, (6) renal functions, and (7) cognitive functions. Though JMDRS has not yet been validated, all MELAS patients had a significantly higher JMDRS score in 2008 than in 2003 (Table 4). Although no differences in the 2003 JMDRS scores were observed between the juvenile and adult forms, the 2008 scores revealed that the juvenile form was associated with a more aggressive deterioration than the adult form. The variation in scores between 2003 and 2008 was much larger in the juvenile form than in the adult form (Table 4).

3.6. Survival curve

Fig. 2 shows the Kaplan–Meier survival curve for MELAS patients. The log-rank analysis showed significant differences in survival between the juvenile and adult forms ($p = 0.0105$). The juvenile

Table 4
Variations of the JMDRS score in the 5-year interval.

	2003	2008	*p* Value
Raw score (minimum = 0, maximum = 81)			
Total ($n=96$)*	4.4 ± 3.2	16.1 ± 9.2	0.0001
Juvenile onset ($n=58$)*	4.9 ± 3.0	19.1 ± 9.7[a]	0.0001
Adult onset ($n=38$)*	3.6 ± 3.5	11.5 ± 6.1[a]	0.006
Score variances between 2003 and 2008			
Total ($n=96$)*	11.8 ± 8.3		
Juvenile onset ($n=58$)*	14.5 ± 8.8[b]		
Adult onset ($n=38$) *	7.8 ± 5.6[b]*Mean ± SD.		

[a] $p=0.0001$, raw scores between the juvenile and adult forms in 2008.
[b] $p=0.0001$, score variances between the juvenile and adult forms.

form had a higher rate of mortality than the adult form (hazard ratio, 3.29; 95%CI, 1.32–8.20).

4. Discussion

In this nationwide, multicenter, 5-year prospective Japanese cohort study, we determined the prevalence of mitochondrial myopathies such as Kearns Sayre syndrome (KSS)/progressive external ophthalmoplegia (PEO), Leigh syndrome, and MELAS. In our study, the prevalence of mitochondrial myopathy was at least 0.58/100,000 in the total population, with MELAS as the most common subtype (data not shown). Although the reported prevalence of mitochondrial disease varies depending on methodology, geography, ethnic group, and subject group, the population-based prevalence of mitochondrial disease risk was 9.18 to 12.48/100,000 in the total population of northeast England [10,11] and [12], 16.5/100,000 in the pediatric population of northeast England [10], 4.7 (95%CI, 2.8–7.6)/100,000 in the pediatric population of western Sweden [13], and 5.0 (95%CI, 4.0–6.2)/100,000 to 13.1/100,000 at birth in Victoria, Australia [14] and [15]. In general, epidemiological studies have estimated that the minimum prevalence of mitochondrial disease is 1/5000 in the general population [16]. The aforementioned prevalence estimates are approximately 10- to 34-fold higher than our estimate (0.58 (95%CI, 0.54–0.62)/100,000 in the total population).

This discrepancy can be explained partly by methodological differences. Because all previously reported prevalence data are based on estimations of risk of mitochondrial diseases extrapolated from the mutation or disease frequency in a limited population or region with regional mitochondrial research institutes or mitochondrial specialists, these values are likely to overestimate the prevalence in the entire population. Whether carriers of pathogenic mitochondrial DNA develop severe mitochondrial disorders depends on the degree and distribution of the mutation in important somatic organs. Although all prevalence studies can contain methodological bias, the prevalence of mitochondrial myopathy should be confirmed by a meta-analysis or nationwide cohort studies in other countries. The discrepancy between our prevalence estimate and previously reported data might also be attributable to a number of additional factors. First, we might have missed some patients due to the imperfect response rate (47%), even though our study included almost all of the main hospitals and institutes in Japan. There was no tendency with respect to region for the lack of responses. However, the response rate for the second questionnaire was significantly different between pediatric and adult neurologists. Pediatric neurologists may not have examined MELAS patients in 2003 although they had examined MELAS patients in 2001; because juvenile MELAS develops at a faster rate than adult MELAS, patients may have died or been referred to an inpatient hospital during 2-year interval. All non-responsive hospitals had less than 300 beds. Generally in Japan, MELAS that is very rare and multi-systematic diseases are monitored in large hospitals that have many departments and beds. Second, it is possible that the mitochondrial myopathies may have been misdiagnosed due to their rarity. Finally, given that most of the prior reports described Caucasian populations, it is possible that the disparity may derive from racial differences. In 2010, the Ministry of Health, Welfare and Labour, Japan has newly approved the mitochondrial myopathy as a supported disorders for their medical expenses, and started to collect the application for such privilege in entire Japan. In above situation, only 100 applications have been collected, to date (personal communication). Because our first questionnaire is also including death case of mitochondrial myopathies, our result come from disease-based prevalence study may be more realistic date at least in Japan.

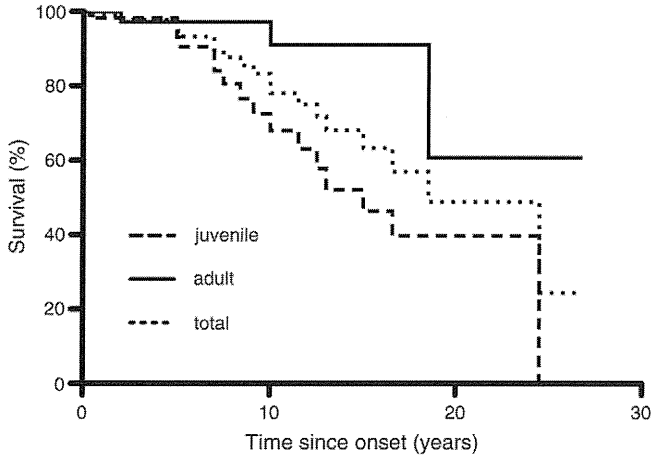

Fig. 2. MELAS survival curve. A Kaplan–Meier survival curve is shown. The dashed line indicates the juvenile form and the solid line indicates the adult form. The results of the log-rank analysis were significant. The juvenile form was associated with a higher risk of mortality than the adult form (hazard ratio, 3.29; 95%CI, 1.32–8.20).

Because MELAS is the most dominant subtype of mitochondrial myopathy and has been associated with an A3243G mutation in the mitochondrial $tRNA^{Leu(UUR)}$ gene, several studies have reported the prevalence of the A3243G mutation. The absolute prevalence of this mutation has been estimated to be as high as 1.41 (95%CI, 0.83–1.20)/100,000 individuals in northern England [12] and [17], 16.3 (95%CI, 11.3–21.4)/100,000 in the adult population of northern Finland [18], and 18.4 (95%CI, 10.9–29.1)/100,000 in the Finnish pediatric population [19]. With the exception of a report from Australia in a large Caucasian population that showed the highest prevalence of 236/100,000 [20], the prevalence of MELAS in Japan (0.18 (95%CI, 0.17–0.19)/100,000) seems to be quite reasonable, given the previously reported prevalence of the A3243G mutation. Because this mutation has been found in association with various clinical conditions, including subclinical asymptomatic carriers and patients with short stature, diabetes mellitus, migraine headache, PEO, MELAS, and/or Leigh syndrome with cardiomyopathy, only individuals whose mutation load in important organs is 50% or more may present with MELAS or a more severe phenotype [21]. Multiple medical problems, including various neurological, cardiological, endocrinological, gastroenterological, and psychiatric symptoms, were reported in 45 families with 45 MELAS patients and 78 carrier relatives in a regional cohort study in the USA [22]. Accordingly, the actual prevalence of the A3243G mutation in human populations may be much higher than previously thought, if we take into account not only the individuals who showed full symptoms of mitochondrial disorders, but also those who show minimal symptoms, even when they were not followed up at a hospital. Nevertheless, MELAS is a clinically and histopathologically defined entity, and the prevalence of MELAS (0.18/100,000 in the total population) in Japan is unlikely to change drastically given more information.

To identify the various symptoms associated with MELAS, we defined the diagnostic criteria for MELAS in Japanese patients. The diagnostic criteria were constructed on the basis of the information provided by Hirano [23] and Hirano and Pavlakis [7]. Category A contains clinical findings of stroke-like episodes, while category B contains evidence of mitochondrial dysfunction. We evaluated only 96 out of 233 MELAS patients. The other patients were excluded for the following reasons; 1) non-response, 2) failure to receive informed consent, 3) patients/neurologists moved to other regions, and 4) other unknown reasons.

According to our data, MELAS can be divided into two subgroups: juvenile and adult forms. This distinction is warranted because of an approximately bimodal distribution of the age of onset, different manifestations of MELAS symptoms in pediatric and adult patients, and differences in the progression of disease as monitored by JMDRS scores. The juvenile form is more severe than the adult form (Tables 2 and 3). No differences in family history were noted between these two forms. However, the juvenile form was associated with significantly higher mortality and a more rapid disease progression than the adult form. We believe that this discrepancy arises because (1) children require more energy to complete their development and maintain their physicality and (2) juvenile patients may have a higher mutation load in mitochondrial genes than in adult patients. Almost all patients with the adult form have a normal life until onset despite having some kind of mitochondrial dysfunction. Therefore, it appears that the adult form requires a longer time for significant symptoms to develop and for the disease to worsen. Because the juvenile form has a greater mutation load than the adult form, it can present more severe complications such as the cardiac and/or renal failure, and patients with the juvenile form are at increased risk of multiple organ failure. Patients with the adult form of MELAS are more likely to have diabetes mellitus and to have a more gradual disease progression. Given these differences in disease progression, our 5-year cohort study may not have provided sufficient time to identify the chronic negative effects of diabetes mellitus especially in the adult form.

Among the clinical symptoms at onset or during the entire course of the disease, seizure and headache were very common and associated with stroke-like episodes in both the juvenile and the adult form. However, of the symptoms present at onset, short stature and failure to thrive were significantly more common in the juvenile form than in the adult form. In contrast, patients with the adult form presented with symptoms such as diabetes mellitus and hearing loss significantly more often than patients with the juvenile form, perhaps because these symptoms are more chronic and maturity (age)-related and can be induced by the accumulation of abnormal mitochondria in low-turnover environments such as pancreatic beta-cells or hearing organs. Of the symptoms encountered during the entire course of the disease, stroke-like episodes were noted in more than 84% of juvenile and adult form patients. Seizure and headache, which are the main symptoms associated with stroke-like episodes, were also common in both juvenile and adult forms. Interestingly, hearing loss, cortical blindness and diabetes mellitus, which are not recognized as main symptoms, were seen significantly more often in the adult form than in the juvenile form. The symptoms listed in our study are consistent with those of previous reports, including the American cohort study [7,8] and [24], the Finnish cohort study [19], and the Japanese muscle biopsy registry of MELAS [5].

We used JMDRS scores to evaluate the progression of MELAS over a 5-year interval. The validated mitochondrial disease rating scale was published in 2006 [25] and [26]. This scale has four classifications, which are age group classification of 0–24 months, 2–11 years, and 12–18 years from the Newcastle pediatric mitochondrial disease scale (NPMDS) [25], and an adult age group classification from the Newcastle mitochondrial disease adult scale (NMDAS) [26]. We had to use the JMDRS although it had not yet been validated because this study started in 2001, and the rating scale was initially mailed to the neurologists in 2003. Contents and indexed factors are similar between NPMDS, NMDAS, and JMDRS. However, NPMDS and NMDAS include contents from patient interviews. This feature is quite different between the Newcastle scales and the JMDRS. In all other respect, the JMDRS is thought to be a comprehensive, quantitative, reproducible, and sensitive monitoring system to detect the progression of disease severity in MELAS. We aimed to use and analyze JMDRS as a pilot study in the present work. According to this analysis, all MELAS patients (both juvenile and adult forms) showed an increased score and worsening of their condition during the 5-year interval. The progression of dysfunction in section 1 (activity of daily living), section 2 (motor activity) and section 7 (cognition and impairment) occurred more rapidly than that in other sections, and it was more pronounced in the juvenile form than in the adult form (data not shown). Patients with more rapidly increasing scores were more commonly found in the group with the juvenile form and had a higher risk of death than those with a more mild disease. This result indicates that the juvenile form progresses more rapidly and is more severe than the adult form. Despite the lack of validation, in this study the JMDRS produced findings that were consistent with a previous study [27] and we believe that the JMDRS is a useful scoring system that allows sensitive and reproducible monitoring of the progression of MELAS. In the future, we will more explicitly validate the JMDRS scoring system for MELAS.

In conclusion, given that no drugs have yet been approved for MELAS, we believe it is important to develop efficacious treatments for MELAS. L-arginine therapy, which is currently in development for MEALS [28], might be a promising drug for the future, and we believe that the results from this study will be helpful for the development of new therapeutic interventions aimed at MELAS.

5. Conclusions

We determined that MELAS occurs into two forms; adult and juvenile, and that the juvenile form is more severe than the adult form. Although our results may contain several biases, including limited information from neurologists, our data highlight new and important information for both pediatric and adult neurologists who are assessing MELAS patients. JMDRS is a useful scoring system for evaluating disease progression in MELAS.

Supplementary materials related to this article can be found online at doi:10.1016/j.bbagen.2011.03.015.

Acknowledgments

All coauthors have seen the manuscript and have reported no conflicts of interest (financial or nonfinancial) and any other pertinent financial information. This work was supported in part by grants #13670853 (Y.K.) and #16390308 (Y.K.) from the Ministry of Culture and Education in Japan, as well as #CCT-B-1803 (Y.K.) from Evidence-based Medicine, Ministry of Health, Labor and Welfare in Japan. S.Y. is a recipient of a post-doctoral fellowship from the Academy of Finland, the Center for International Mobility in Finland. N.P. is a recipient of a grant-in-aid for young investigators from the Heiwa Research Foundation in Japan.

The authors express thanks to the following investigators of the MELAS study group in Japan for participating in the nationwide cohort study and providing important information on MELAS patients: Drs. Hideki Hozen (Obihiro), Muneaki Matsuo (Saga), Atsushi Yamagishi (Takayama), Yasushi Otsuka (Toki), Shinji Saitoh (Sapporo), Takahiro Iizuka (Sagamihara), Tomoyuki Takano (Otsu), Shuji Hashiguchi (Yoshinogawa), Akihiko Ogata (Sapporo), Nobuya Fujita (Nagaoka), Kazuyuki Yotsumoto (Kagoshima), Ken Sakurai (Tokyo), Taro Matsuoka (Toyonaka), Megumi Nakanishi (Kahoku), Yukihiro Shikama (Kahoku), Kimihiko Yoshimura (Kochi), Takao Soda (Izumisano), Susumu Ito (Kita), Takuma Iwaki (Kita), Tetsuya Ito (Nagoya), Akira

Sudo (Sapporo), Hiroyuki Torisu (Fukuoka), Minako Kihara (Kyoto), Shuji Kishida (Tokyo), Akiko Ishii (Tsukuba), Kenji Fujishima (Tokyo), Hisashi Kawawaki (Osaka), Shin Okazaki (Osaka), Hiroyuki Watanabe (Nagaoka), Kazumasa Shindo (Chuo), Yasuhisa Toribe (Izumi), Yukiko Mogami (Izumi), Keiko Yanagihara (Izumi), Go Tajima (Hiroshima), Atsuko Noguchi (Akita), Etsuo Naito (Tokushima), Kazuhiro Oginoya (Sendai), Masataka Kitaguchi (Sakai), Sadayuki Nukina (Akashi), Kazutoshi Nakano (Tokyo), Yoshihide Sunada (Kurashiki), Hitoshi Sejima (Izumo), Yasumasa Ohyagi (Fukuoka), Muneichiro Sumi (Omura), Tomoaki Yuhi (Kitakyushu), Mitsue Fujita (Tsukuba), Yasuto Higashi (Himeji), Makoto Yoneda (Yoshida), Masanori Nakagawa (Kyoto), Ritsuko Shigemi (Matsuyama), and Hidee Arai (Chiba).

References

[1] R.W. Taylor, D.M. Turnbull, Mitochondrial DNA mutations in human disease, Nat. Rev. Genet. 6 (2005) 389–402.

[2] S.G. Pavlakis, P.C. Phillips, S. DiMauro, D.C. De Vivo, L.P. Rowland, Mitochondrial myopathy, encephalopathy, lactic acidosis, and stroke like episodes: a distinctive clinical syndrome, Ann. Neurol. 16 (1984) 481–488.

[3] S. DiMauro and M. Hirano. MELAS, R.A. Pagon, T.C. Bird, C.R. Dolan, K. Stephens and editors, Seattle (WA), University of Washington Seattle, *Gene reviews* [Internet; http://www.ncbi.nlm.nih.gov/books/NBK1233/] (1993), updated 2010 Oct 14.

[4] Y. Goto, I. Nonaka, A. Horai, A mutation in the tRNA(Leu)(UUR) gene associated with the MELAS subgroup of mitochondrial encephalomyopathies, Nature 348 (1990) 651–653.

[5] Y. Goto, S. Horai, T. Matsuoka, Y. Koga, K. Nihei, M. Kobayashi, I. Nonaka, Mitochondrial myopathy, encephalopathy, lactic acidosis, andstrokelike episodes (MELAS): a correlative study of the clinical features and mitochondrial DNA mutation, Neurology 42 (1992) 545–550.

[6] J.M. van den Ouweland, H.H. Lemkes, K.D. Gerbitz, J.A. Maassen, Maternally inherited diabetes and deafness (MIDD): a distinct subform of diabetes associated with a mitochondrial tRNA(Leu)(UUR) gene point mutation, Muscle Nerve 3 (1995) S124–130.

[7] M. Hirano, S.G. Pavlakis, Mitochondrial myopathy, encephalopathy, lactic acidosis, andstrokelike episodes (MELAS): current concepts, J. Child Neurol. 9 (1994) 4–13.

[8] D.M. Sproul, P. Kaufmann, Mitochondrial encephalopathy, lactic acidosis, and strokelike episodes, basic concepts, clinical phenotype, and therapeutic management of MELAS syndrome, Ann. N.Y. Acad. Sci. 1143 (2008) 133–158.

[9] P.F. Chinnery, L.A. Bindoff, 116th ENMC international workshop: the treatment of mitochondrial disorders, 14th–16th March 2003, Naarden, The Netherlands, Neuromuscul. Disord. 13 (2003) 757–764.

[10] A.M. Schaefer, R. McFarland, E.L. Blakely, L. He, R.G. Whittaker, R.W. Taylor, P.F. Chinnery, D.M. Turnbull, Prevalence of mitochondrial DNA disease in adults, Ann. Neurol. 63 (2008) 35–39.

[11] A.M. Schaefer, R.W. Taylor, D.M. Turnbull, P.F. Chinnery, The epidemiology of mitochondrial disorders—past, present and future, Bioch. Biophy. Act BBA Bioenerg. 1659 (2004) 115–120.

[12] P.F. Chinnery, M.A. Johnson, T.M. Wardell, R. Singh-Kler, C. Hayes, D.T. Brown, R.W. Taylor, L.A. Bindoff, D.M. Turnbull, The epidemiology of pathogenic mitochondrial DNA mutations, Ann. Neurol. 48 (2000) 188–193.

[13] N. Darin, A. Oldfors, A.R. Moslemi, E. Holme, M. Tulinius, The incidence of mitochondrial encephalomyopathies in childhood: clinical features and morphological, biochemical, and DNA abnormalities, Ann. Neurol. 49 (2001) 377–383.

[14] D. Skladal, J. Halliday, D.R. Thorburn, Minimum birth prevalence of mitochondrial respiratory chain disorders in children, Brain 126 (2003) 1905–1912.

[15] D.R. Thorburn, Mitochondrial disorders: prevalence, myths and advances, J. Inher. Metab. Dis. 27 (2004) 349–362.

[16] H.R. Elliott, D.C. Samuels, J.A. Eden, C.L. Relton, P.F. Chinery, Pathogenic mitochondrial DNA mutations are common in the general population, Am. J. Hum. Genet. 83 (2008) 254–260.

[17] P.F. Chinnery, D.M. Turnbull, Epidemiology and treatment of mitochondrial disorders, Am. J. Med. Genet. 106 (2001) 94–101.

[18] K. Majamaa, J.S. Moilanen, S. Uimonen, A.M. Remes, P.I. Salmela, M. Kärppaä, K.A. Majamaa-Voltti, H. Rusanen, M. Sorri, K.J. Peuhkurinen, I.E. Hassinen, Epidemiology of A3243G, the mutation for mitochondrial encephalomyopathy, lactic acidosis, and strokelike episodes: prevalence of the mutation in an adult population, Am. J. Hum. Gen. 63 (1998) 447–454.

[19] J. Uusimaa, J.S. Moilanen, L. Vainionpää, P. Tapanainen, P. Lindholm, M. Nuutinen, T. Löppönen, E. Mäki-Torkko, H. Rantala, K. Majamaa, Prevalence, segregation, and phenotype of the mitochondrial DNA 3243A>G mutation in children, Ann. Neurol. 62 (2007) 278–287.

[20] N. Manwaring, M.M. Jones, J.J. Wang, E. Rocthchina, C. Howard, P. Mitchell, C.M. Sue, Population prevalence of the MELAS A3243G mutation, Mitochondrion 7 (2007) 230–233.

[21] Y. Koga, Y. Akita, N. Takane, Y. Sato, H. Kato, Heterogeneous presentation in A3243G mutation in the mitochondrial tRNALeu(UUR) gene, Arch. Dis. Child. 82 (2000) 407–411.

[22] P. Kaufmann, K. Engelstad, Y. Wei, R. Kulikova, M. Oskoui, V. Battista, D.Y. Koenigsberger, J.M. Pascual, M. Sano, M. Hirano, S. DiMauro, D.C. Shungu, X. Mao, D.C. DeVivo, Protean phenotypic features of the A3243G mitochondrial DNA mutation, Arch. Neurol. 66 (2009) 85–91.

[23] M. Hirano, E. Ricci, M.R. Koenigsberger, R. Defendini, S.G. Pavlakis, D.C. Devivo, S. Diauro, L.P. Rowland, Melas: an original case and clinical criteria for diagnosis, Neuromuscul. Disord. 2 (1992) 125–135.

[24] D.M. Sproule, P. Kaufmann, K. Engelstad, T.J. Starc, A.J. Hordof, D.C. De Vivo, Wolff–Parkinson–White syndrome in patients with MELAS, Arch. Neurol. 64 (2007) 1625–1627.

[25] C. Phoenix, A.M. Schaefer, J.L. Elson, E. Morava, M. Bugiani, G. Uziel, J.A. Smeitink, D.M. Turnbull, R. McFarland, A scale to monitor progression and treatment of mitochondrial disease in children, Neuromuscul. Disord. 16 (2006) 814–820.

[26] A.M. Scheafer, C. Phoenix, J.L. Elson, R. McFarland, P.F. Chinnery, D.M. Turnbull, Mitochondrial disease in adults; A scale to monitor progression and treatment, Neurology 66 (2006) 1932–1934.

[27] D. Skladal, V. Sudmeier, S. Konstantopoulou, S. Stöckler-Ipsiroglu, B. Plecko-Startinig, G. Bernert, J. Zeman, W. Sperl, The spectrum of mitochondrial disease in 75 pediatric patients, Clin. Pediatr. 42 (2003) 703–710.

[28] Y. Koga, N. Povalko, J. Nishioka, K. Katayama, N. Kakimoto, T. Matsuishi, MELAS and L-arginine therapy: pathophysiology of stroke-like episodes, Ann. NY Acad. Sci. 1201 (2010) 104–110.

Original Paper

European Neurology

Eur Neurol 2012;67:232–237
DOI: 10.1159/000336568

Received: August 8, 2011
Accepted: January 14, 2012
Published online: March 14, 2012

Evaluation of Systemic Redox States in Patients Carrying the MELAS A3243G Mutation in Mitochondrial DNA

Masamichi Ikawa[a] Kenichiro Arakawa[b] Tadanori Hamano[a] Miwako Nagata[c]
Yasunari Nakamoto[a] Masaru Kuriyama[a] Yasutoshi Koga[d] Makoto Yoneda[a]

[a]Second Department of Internal Medicine, and [b]Department of Cardiology, Faculty of Medical Sciences, University of Fukui, and [c]Department of Neurology, Nakamura Hospital, Fukui, and [d]Department of Pediatrics and Child Health, Kurume University School of Medicine, Fukuoka, Japan

Key Words
MELAS · A3243G mutation · Mitochondrial DNA · Oxidative stress · Antioxidant activity · Redox states · d-ROMs test · BAP test

Abstract
Background/Aims: To clarify the change of systemic redox states in patients carrying the A3243G mutation in mitochondrial DNA (A3243G), we evaluated oxidative stress and antioxidant activity in the serum of patients. ***Methods:*** Oxidative stress and antioxidant activity in the serum samples obtained from 14 patients carrying A3243G and from 34 healthy controls were analyzed using the diacron-reactive oxygen metabolites (d-ROMs) and biological antioxidant potential (BAP) tests, respectively. ***Results:*** The mean d-ROMs level of all patients was significantly greater than that of the controls ($p < 0.005$), and the mean BAP/d-ROMs ratio of all patients was significantly lower than that of the controls ($p < 0.02$). In the patients with a history of stroke-like episodes ($n = 10$), both mean d-ROMs and BAP levels were increased compared with those of the controls (both $p < 0.01$). The mean BAP level of the patients without a history of stroke-like episodes ($n = 4$) was significantly decreased compared with that of the controls ($p < 0.001$), but the mean d-ROMs levels were not significantly different. ***Conclusion:*** d-ROMs and BAP tests indicated that patients carrying A3243G are always exposed to underlying oxidative stress, even at a remission state of stroke-like episodes.

Introduction

Mitochondrial myopathy, encephalopathy, lactic acidosis and stroke-like episodes (MELAS) syndrome is the most common type of mitochondrial disease, and is mainly caused by an A-to-G transition mutation at nucleotide position 3243 (A3243G) in mitochondrial DNA (mtDNA) [1]. MELAS is characterized by stroke-like episodes that occur repeatedly and provoke neurological symptoms (e.g. headache, epilepsy, hemiparesis, and dementia) due to 'stroke-like' brain lesions [2]. In other words, stroke-like episodes are diagnostic symptoms of MELAS, and are crucial factors determining the prognosis of patients with this syndrome [2].

In addition, A3243G is responsible for not only stroke-like episodes but also mitochondrial cardiomyopathy or diabetes mellitus (DM) [1, 3–6]. Conversely, some patients carrying A3243G present with typical MELAS syn-

KARGER

Fax +41 61 306 12 34
E-Mail karger@karger.ch
www.karger.com

0014–3022/12/0674–0232$38.00/0

Accessible online at:
www.karger.com/ene

Makoto Yoneda, MD, PhD
Second Department of Internal Medicine
Faculty of Medical Sciences, University of Fukui
23-3 Shimoaiduki, Matsuoka, Eiheiji-cho, Fukui 910-1193 (Japan)
Tel. +81 776 61 8351, E-Mail myoneda@u-fukui.ac.jp

Table 1. Demographic characteristics of patients and controls

Subject	Patients			Normal controls
	all	'stroke type'	'non-stroke type'	
Number	14	10	4	34
Gender (males/females)	7/7	5/5	2/2	20/14
Mean age at examination, years	32.1 ± 14.7	27.8 ± 12.5	42.8 ± 15.8	34.6 ± 7.4
Clinical features				
Stroke-like episodes, n	10	10	0	0
Cardiomyopathy, n	6	2	4	0
Diabetes, n	3	0	3	0
Under antioxidant therapy, n	11	10	1	0

Values are mean ± SD.

dromes with stroke-like episodes, and others present with only cardiomyopathy or DM without stroke-like episodes. However, the pathophysiological difference of phenotypes between the presence and absence of stroke-like episodes in patients carrying A3243G remains obscure.

Recent studies using cells cultured in vitro demonstrated increased oxidative stress in cells with impaired mitochondria due to A3243G [7–10]. Oxidative stress is provoked by reactive oxygen species (ROS) generation exceeding antioxidant defenses, such as manganese superoxide dismutase and glutathione peroxidase, and damages nucleic acids, proteins and lipids, which leads to cellular dysfunction. Indeed, previous pathological or imaging studies demonstrated enhanced regional oxidative stress in lesions of both stroke-like episodes and cardiomyopathy in patients carrying A3243G [11–13]. Therefore, there is a high possibility that oxidative stress participates in the pathogenesis caused by A3243G, and influences the phenotypic diversity. In other words, redox (reduction-oxidation) states should be evaluated in patients carrying A3243G both with and without a history of stroke-like episodes to clarify the role of oxidative stress in the emergence of stroke-like episodes.

To perform such an investigation, a rapid and reliable method of evaluating redox states in patients carrying A3243G is needed. Direct measurement of oxidative stress and antioxidant activity in living humans has been difficult; redox states have thus not been clearly evaluated in patients carrying A3243G to date. Recently, the diacron-reactive oxygen metabolites (d-ROMs) and biological antioxidant potential (BAP) tests have been used to evaluate redox states in serum. The d-ROMs level reflects the intensity of oxidative stress, and the BAP level indicates the activity of endogenous antioxidants [14, 15]. Their effectiveness as clinical markers has been reported in various diseases [16–22]. We evaluated redox states in fresh serum of both patients carrying A3243G and healthy volunteers using d-ROMs and BAP tests, and clarified the change of redox states due to A3243G and the pathophysiological difference in phenotypes with or without stroke-like episodes.

Subjects and Methods

Subjects

Fourteen Japanese patients (7 men and 7 women; mean age 32.1 ± 14.7 years) carrying A3243G were recruited at the University of Fukui Hospital, Fukui, and at the Kurume University Hospital, Fukuoka, Japan (table 1). Patients were classified by the presence or absence of stroke-like episodes into 'stroke type' and 'non-stroke type'. Ten patients with a history of stroke-like episodes were categorized as 'stroke type', and the other 4 patients who presented with mainly cardiomyopathy without a history of stroke-like episodes were categorized as 'non-stroke type'. Eleven patients were treated by antioxidant therapy such as coenzyme Q_{10} (CoQ_{10}; daily dose 30–90 mg) and/or vitamin E (daily dose 100 mg) administration; 10 of these patients were 'stroke type', and the other patient was 'non-stroke type'. Eight patients categorized as 'stroke type' were also treated with an oral administration of L-arginine (daily dose 14–21 g). All patients were in remission, free from exacerbation of symptoms or acute stroke-like episodes, when they were examined. Functional status was evaluated using the performance status rating (mean rating 1.3 ± 1.0). In 'stroke type' patients, the mean age of the first stroke-like episode was 21.1 ± 15.2 years, and the mean duration between the examination and the last stroke-like episode was 14.2 ± 9.2 months. 'Stroke type' patients had headaches and/or vomiting on average twice a month, but almost none had convulsions. Thirty-four Jap-

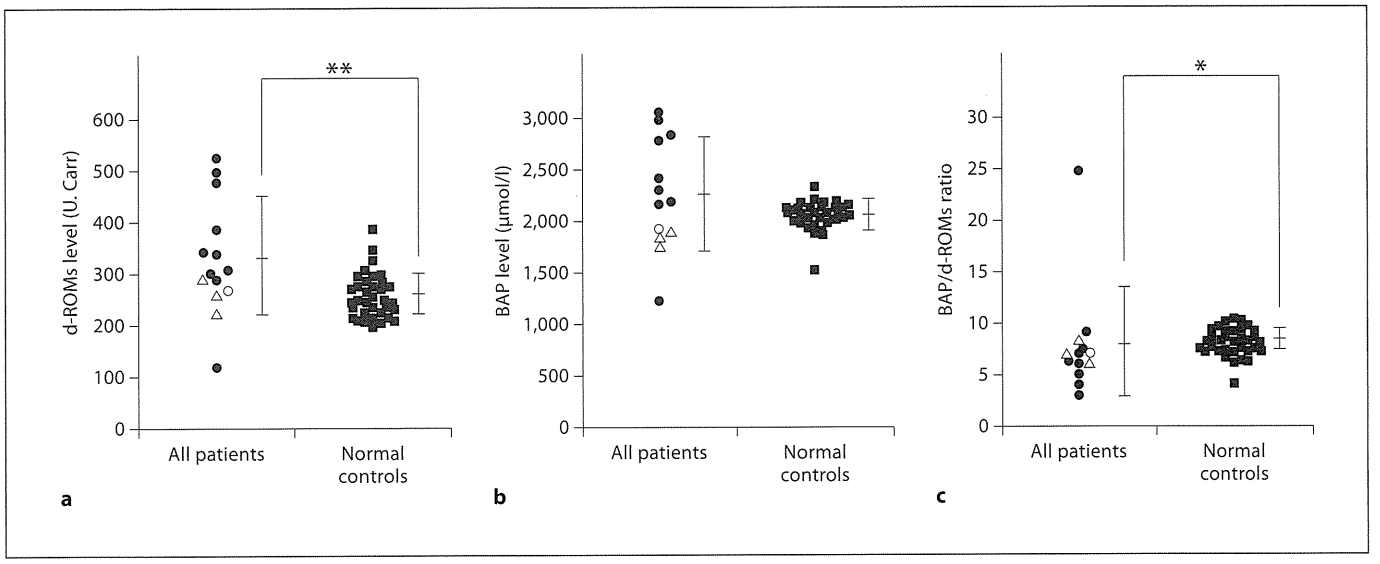

Fig. 1. Scatter plots portraying the levels of d-ROMs (**a**) and BAP (**b**) and BAP/d-ROMs ratios (**c**) in all the patients and controls. Circles and triangles correspond to the patients with and without antioxidant administration, respectively. In addition, closed and open diagrams correspond to the 'stroke type' patients and 'non-stroke type' patients, respectively. * $p < 0.02$, ** $p < 0.005$, according to the two-tailed Mann-Whitney U test. Bars indicate mean ± SD.

anese healthy volunteers (20 men and 14 women; mean age 34.6 ± 7.4 years) were also recruited as normal controls from the local community (table 1). This study was approved by the Ethics Committee of the University of Fukui. All subjects provided written informed consent to participate in the study.

Measurement of Oxidative Stress Levels

The oxidative stress levels were evaluated by measuring the quantity of hydroperoxides (R-OOH) in fresh serum samples using the d-ROMs test with the Free Radical Analytical System 4 (FRAS4^R; H&D srl, Parma, Italy) automatically [14]. Blood sampling was performed at fasting and at rest. Hydroperoxides consist of dehydrogenized and peroxidized proteins, lipids and fatty acids produced by ROS. In the d-ROMs test, hydroperoxides are turned to radicals by the Fenton reaction in an acid medium, and these generated radicals oxidize *N,N*-diethyl-paraphenylenediamine (DEPPD). Oxidized DEPPD quantity is determined by an absorbency measurement (white light 505 nm). The sequence of these methods is automated, and oxidative stress levels can be evaluated easily and quickly. The values are expressed as U. Carr, where 1 U. Carr corresponds to 0.8 mg/l H_2O_2.

Measurement of Antioxidant Activity Levels

The antioxidant activity levels were evaluated by measuring the quantity of molecules with antioxidative potency in fresh serum samples using the BAP test in the FRAS4^R automatically [15, 17]. Blood sampling was performed at fasting and at rest. In the BAP test, serum molecules with antioxidative potency reduce and decompose compounds of ferric chloride ($FeCl_3$) and thiocyanate derivative (AT) to $FeCl_2$ and free AT. Free AT is achromatized and dissociates from compounds, and is quantified by an absorbency measurement (white light 505 nm). The sequence of these methods is automated, and antioxidant activity levels can be evaluated easily and quickly. The results are expressed as μmol/l.

Statistical Analysis

The BAP-to-d-ROMs ratio (BAP/d-ROMs ratio) was calculated from the ratio of the BAP levels and d-ROMs levels for each subject. Data are presented as means ± standard deviations (SD). The resultant differences between normal controls and all patients were analyzed by means of a two-tailed Mann-Whitney U test. Since the subject number of each group was small, a non-parametric Kruskal-Wallis test was used for multiple data comparison and a post hoc Dunn test was performed to evaluate differences among normal controls, 'stroke type' patients and 'non-stroke type' patients. All statistical analyses were performed in SPSS Statistics Version 17.0 (SPSS Japan Inc., Tokyo, Japan), and $p < 0.05$ was considered significant.

Results

The levels of serum d-ROMs and BAP, and BAP/d-ROMs ratios of all the patients and controls are shown in figure 1, and those of the 'stroke type' patients, 'non-stroke type' patients and controls are shown in figure 2. The mean age of each group demonstrated no significant differences.

The mean d-ROMs level of all patients (332.6 ± 110.7 U. Carr) was significantly higher than that of the controls